HHS Public Access

Author manuscript

Nat Metab. Author manuscript; available in PMC 2021 June 07.

Published in final edited form as:

Nat Metab. 2020 December ; 2(12): 1459–1471. doi:10.1038/s42255-020-00312-4.

Nitrogen recycling buffers against ammonia toxicity from skeletal muscle breakdown in hibernating arctic ground squirrels

Sarah A. Rice[1,2], **Gabriella A.M. ten Have**[4], **Julie A. Reisz**[3], **Sarah Gehrke**[3], **Davide Stefanoni**[3], **Carla Frare**[1,2], **Zeinab Barati**[1,2], **Robert H. Coker**[2], **Angelo D'Alessandro**[3], **Nicolaas E.P. Deutz**[4], **Kelly L. Drew**[1,2,*]

[1]Department of Chemistry and Biochemistry, University of Alaska Fairbanks

[2]Institute of Arctic Biology, Center for Transformative Research in Metabolism, University of Alaska Fairbanks

[3]Department of Biochemistry and Molecular Genetics, University of Colorado Anschutz Medical Campus

[4]Center for Translational Research in Aging and Longevity, Department of Kinesiology, Texas A&M University

Abstract

Hibernation is a state of extraordinary metabolic plasticity. The pathways of amino acid metabolism as they relate to nitrogen homeostasis in hibernating mammals *in vivo* is unknown. Here we show, using pulse isotopic tracing, evidence of increased myofibrillar (skeletal muscle) protein breakdown and suppressed whole body production (WBP) of metabolites *in vivo* throughout deep torpor. As WBP of metabolites is suppressed, amino acids with nitrogenous side chains accumulate over torpor while production of urea cycle intermediates do not. Using ^{15}N stable isotope methodology in arctic ground squirrels (*Urocitellus parryii*), we provide evidence that free nitrogen is buffered and recycled into essential amino acids (EAA), non-essential amino acids (NEAA), and the gamma-glutamyl system during the interbout arousal period of hibernation. In the absence of nutrient intake or physical activity, our data illustrate the orchestration of metabolic pathways that sustain the provision of essential and non-essential amino acids and prevent ammonia toxicity during hibernation.

*Corresponding Author: kdrew@alaska.edu.

Author contribution: SR, KD, GT, AD, RC and ND conceived the project and designed the research. SR and CF performed the experiments. GT, ND, JR, SG, SR, DS, ZB analyzed the data and samples. SR wrote the manuscript with intellectual input from all authors.

Competing Interests: SR, AD, JR, SG, DS, CF, GT, and ND have no competing interests declared. KLD has a financial interest in Be Cool Pharmaceutics. RHC has a financial interest in Essential Blends, LLC. ZB has a financial interest in Barati Medical, LLC.

Data Availability: The datasets generated during and/or analyzed during the current study are available from the corresponding author on reasonable request.

Introduction:

Hibernation is a state of extreme metabolic and physiologic plasticity that occurs in conjunction with physical inactivity and prolonged fasting.[1] Specifically, hibernating Arctic Ground Squirrels (AGS) fast for up to eight months without any exogenous nitrogen intake, yet they are able to maintain physiological function and skeletal muscle.[2–4] Urea nitrogen salvage with nitrogen recycling into amino acids has been hypothesized for decades as a major mechanism to support anabolic processes while preserving protein content in hibernation.[5–8] Less focus has been devoted to free nitrogen. The nature of protein degradation, and how hibernating ground squirrels maintain nitrogen homeostasis and utilize free nitrogen to preserve amino acid stores, has remained unknown due to technical limitations of measuring *in vivo* fluxes in deep torpor.

Hibernation in AGS is composed of torpor bouts (approximately fourteen to twenty days long) where the whole body metabolic rate is reduced to 1-2 percent of basal metabolic rate and core body temperature (T_b) can dip below 0°C.[3,9] Torpor bouts are interrupted by naturally occurring interbout arousals, with a duration of 12-24 hours.[10] As torpor progresses, amino acids with nitrogenous side chains accumulate in tissues of ground squirrels, signifying increased nitrogen load.[11,12] Multiple tissues, ranging from skeletal muscle, kidney, liver, small intestine, lung and brain, contribute to systemic nitrogen homeostasis, ammonia detoxification and sequestration of nitrogen into amino acids.[13–15] There is evidence anabolism occurs in liver and small intestine during hibernation, which is dependent on recycling of nitrogen into protein.[7] Several other studies indicate a capacity of hibernators to recycle nitrogen, but most have focused on microbial urea nitrogen salvage.[6–8] Nitrogen recycling into non-essential and essential amino acids in hibernating bears (n=2) was measured in a preliminary study using a $^{15}N_2$ urea tracer.[16] This tracer formed ^{15}N ammonia in plasma, indicating that metabolic pathways facilitating recycling could use either urea or free ammonia.[16] Previous studies have demonstrated that the levels of circulating ammonia remain constant throughout torpor but it is unknown how ammonia is utilized in nitrogen salvage.[12,17]

While hypothesized to derive from breakdown of labile tissues,[18] the source of circulating free amino acids and free nitrogen in hibernation is unknown. No study to our knowledge has measured *in vivo* production rates of protein degradation markers or amino acids in deep torpor. Further, the metabolic pathways and tissues that facilitate nitrogen buffering and recycling of amino acids are unknown.

We tested the hypothesis that breakdown of skeletal muscle during torpor contributes to free nitrogen load and that this load is buffered through transamination reactions involving multiple tissues. Our approach included a pulse infusion of a tracer cocktail containing amino acids and metabolites in deep torpor and summer (Fig. 1).[19] In addition we performed metabolomic analysis on blood sampled from indwelling arterial cannula throughout entrance, torpor and arousal and we traced the fate of ^{15}N following infusion of ^{15}N ammonium acetate during arousal from torpor in AGS.

Results:

Skeletal muscle breakdown continues albeit at a slow rate in deep torpor

Tau-methylhistidine (3-MH) is a skeletal muscle degradation marker and *trans*-4-hydroxy-L-proline (hPRO) is a collagen degradation marker.[20,21] We found decreases in both 3-MH and hPRO whole body production (WBP) in torpor compared to summer euthermia (Fig. 2a, table insert, $p<0.001$, t-tests), but the relative reduction of 3-MH was significantly less than hPRO (Fig. 2a, $p<0.001$, t-test). Specifically, hPRO WBP is reduced to 1% of euthermic rates, which reflects the overall 98% reduction in whole body metabolism during AGS torpor,[9] while 3-MH is reduced to only 22% of euthermic levels. In normal physiology, collagen turnover is far higher than skeletal muscle turnover,[21,22] as is seen in our euthermic summer animals where hPRO WBP is 8.27 (nmol/g body weight/hr) compared to 3-MH WBP of 1.83 (nmol/g body weight/hr). Conversely, in deep torpor 3-MH WBP (0.41 nmol/g body weight/hr) is approximately three times higher than hPRO WBP (0.13 nmol/g body weight/hr).

The reduced suppression of 3-MH WBP compared to hPRO WBP indicates that myofibrillar (skeletal muscle) breakdown occurs throughout torpor, albeit at a low rate.

Skeletal muscle breakdown may be a source of amino acids in torpor

WBP of all amino acids indicate profound suppression of metabolic processes in deep torpor compared to summer (Fig. 2b, $p<0.05$, paired t-tests, FDR corrected), however, the degree of suppression varied between amino acids (Fig. 2c).

Since our findings show that skeletal muscle degradation is ongoing during torpor, we next asked if amino acid production correlated with skeletal muscle breakdown. Regression analysis showed significant linear relationships between WBP rates of 3-MH in deep torpor and WBP of glutamine, phenylalanine and citrulline (Figure 2d). The linear relationship between rates of WBP of 3-MH and WBP of phenylalanine and glutamine in torpor argue that these amino acids originate from skeletal muscle during torpor. Further, given that glutamine is a precursor to citrulline synthesis in the gut the correlation between citrulline and 3-MH WBP suggests that small intestine metabolism may be linked to glutamine release from skeletal muscle during deep torpor.

Nitrogen carriers accumulate over deep torpor with a lack of kidney metabolic recycling

Previous metabolic profiling in other hibernating species shows that plasma levels of certain amino acids deplete or accumulate as torpor progresses.[11,23–25]

We observed an increase in plasma glutamine, alanine and glutamate as torpor progressed over approximately two weeks (Fig. 3, $n=9$, glutamate $p<0.034$, glutamine $p<0.001$, alanine $p<0.001$, repeated measures ANOVA). The accumulation of glutamine in liver and brain over torpor in other species support our finding of increased nitrogen load as torpor progresses.[11,12] While some previous plasma metabolomic studies do not mention a significant increase in glutamine or glutamate between entrance and late torpor, it is

important to note that we evaluated these changes with high resolution, longitudinal sampling within animals.[23,25]

We also observed that urea cycle intermediates (arginine, ornithine, citrulline) do not increase over torpor (Fig. 3, n=9), consistent with prior evidence that the urea cycle is suppressed during torpor.[12,17,26] Ammonia, present in plasma throughout torpor, is naturally released during amino acid catabolism following protein degradation.[12,17,27] Ammonia is typically incorporated into urea in the liver, but another major pathway for sequestering free nitrogen is via glutamine synthetase (GS) to form glutamine as the major nitrogen carrying amino acid, which occurs in multiple tissue types and skeletal muscle.[13–15,27,28] Thus, our results support a model whereby free nitrogen released during protein breakdown and catabolism accumulates in glutamine, glutamate, and alanine (products of transamination).

Multiple waste byproducts of amino acid and purine catabolism, such as creatine, creatinine, and hPRO or hypoxanthine, allantoin and xanthine also increased, respectively (Fig. 3, n=9, $p<0.05$ for each of these metabolites, repeated measures ANOVA). We interpret the accumulation of metabolites, such as creatinine, as evidence of amino acid catabolism throughout torpor as well as reduction in the kidney glomerular filtration rate (GFR), also supported by prior studies (Fig. 3).[26,29] Accumulation of collagen breakdown products such as hPRO illustrates that production outpaces reabsorption or recycling during torpor. In total, these results suggest low-grade catabolism paired with reduced kidney function and accumulating nitrogen load with flux into non-essential amino acids instead of urea cycle intermediates. Alternatively, urea cycle intermediates may not accumulate due to loss via microbial urease enzyme activity.[8] We next asked if AGS lessen the nitrogen load through metabolic recycling and anabolic metabolism once these processes resume during the interbout arousal period.

Nitrogen fluxes into metabolites during arousal from torpor

To understand how free nitrogen liberated from protein breakdown is incorporated into amino acids and metabolic pathways we next measured enrichment of ^{15}N derived from ^{15}N ammonium acetate infused during interbout arousal. We traced nitrogen incorporated into multiple metabolites in plasma and tissues (Fig. 4). Overall ^{15}N ammonia incorporated into non-essential amino acids (NEAA) (glutamine, alanine, glutamate, arginine, asparagine, proline, serine, citrulline and ornithine) as well as essential amino acids (EAA) (leucine-isoleucine, valine, threonine, histidine) and the gamma-glutamyl intermediate 5-oxoproline (Fig. 4). All tissues incorporated free ^{15}N into metabolic pathways (Fig. 4). ^{15}N incorporation from ammonium acetate into EAA and NEAA supports de novo synthesis.

Notably, we found significant incorporation of ^{15}N into glutamate in plasma (44.6±4.66% of total Glu), liver (13.5±3.7%), kidney (7.9±1.8%), skeletal muscle (0.7 ±0.2%), small intestine (1.4±0.3%) and lung (2.3±0.6%) (reported here as mean±SEM and denoted as M +1, Fig. 5). The majority of our proposed pathways for ammonia ^{15}N incorporation during arousal from torpor stem first from synthesis of ^{15}N glutamate indicating a central role of this metabolite in hibernation nitrogen homeostasis. Previous in vitro studies suggest the reversibly phosphorylated glutamate dehydrogenase (GDH), which can incorporate free nitrogen into glutamate, catalyzes primarily the reverse reaction, glutamate oxidation, during

hibernation.[30,31] GDH, however, has complex, strong allosteric regulators[32] and our data shows a clear ability of ^{15}N to be incorporated into glutamate, indicating in vivo activity of this enzyme to generate glutamate in AGS hibernation. ^{15}N Enrichment of urea cycle intermediate ornithine was observed in the small intestine, but the percent of ^{15}N incorporation is less than other metabolites in this tissue (Fig. 5).

^{15}N Incorporation into glutamate and arginosuccinate suggest that glutamate is a major contributor to ^{15}N-argininosuccinate and ^{15}N-arginine synthesis through ^{15}N-aspartate. ^{15}N-Aspartate was observed in liver (12.3±3.2%), plasma (29.3±6.3%), kidney (7.5±1.2%) and lung (2.1±0.6%) (Fig. 5). ^{15}N-Argininosuccinate was observed in liver (4.9±1.4%) and ^{15}N-arginine was observed in plasma (0.4±0.1%) and kidney (0.2±0.1%) (Fig. 5). Many of these synthesized NEAAs are direct protein precursors and exert protein anabolic effects, which represent metabolic pools available to stimulate protein synthesis during arousal to counteract skeletal muscle breakdown during torpor.[27,33] Recent metabolic modeling predicted increased NEAA synthesis in grizzly bears.[34] These findings also support previous work suggesting that amino acid anabolism is upregulated[4] and nitrogen is redeposited in liver and small intestine during AGS hibernation.[7]

^{15}N Incorporated into leucine-isoleucine, threonine, and histidine suggests that ^{15}N-glutamate contributes to the synthesis of branched chain amino acids (BCAA) and essential amino acids (EAA). De novo EAA synthesis in hibernation has been proposed in the hibernating bear,[16] a notion that has been challenged by subsequent studies suggesting that de novo EAA synthesis might not be required due to readily available EAA resources in labile proteins that can be catabolized over the season.[35,36] Incorporation of ^{15}N into leucine-isoleucine in kidney was 4.6±1.0% (Fig. 5). ^{15}N-Glutamate is abundant in kidneys and glutamate donates nitrogen to branched-chain amino acid aminotransferases (BCAT), which catalyze nitrogen incorporation/removal between BCAAs and their α-keto acid analogues which are typically rich in kidney.[37] A previous study in dogs revealed renal ability to reincorporate nitrogen into leucine's keto-acid, supporting this capability in mammals.[38] Exceptionally reduced renal glomerular filtration rate (GFR) in torpor is reversed with the return of kidney function during interbout arousal.[26,29,39] Further, proteomic analysis of ground squirrel kidneys show that BCAA catabolism proteins decrease in hibernation[40] and isotopic leucine tracer studies in black bears indicate very low levels of oxidized leucine in hibernation.[41] Taken together with these studies, our data indicates that renal hibernation BCAA metabolism is shifted toward anabolism rather than catabolism. Further, ^{15}N incorporation into leucine correlated significantly, or near significantly, with T_b in kidney, lung, plasma and skeletal muscle illustrating the temperature dependence of this process (Extended Fig. 2). Incorporation of ^{15}N glutamine also varied with temperature in some tissues (Extended Fig. 4–5). ^{15}N Incorporation into glutamate only correlated with T_b in muscle (Extended Fig. 3). ^{15}N Incorporation into valine (Extended Fig. 6) did not correlate with temperature in any tissue studied. This evidence suggests that rising T_b facilitates nitrogen incorporation into some BCAA in multiple tissues.

^{15}N-Glutamate and ^{15}N-aspartate are also precursors to ^{15}N-threonine. ^{15}N Incorporation into threonine was observed in plasma (1.7±0.5%), liver (1.6±0.2%), kidney (0.5±0.2%), small intestine (1.6±0.2%) and lung (1.0±0.2%) (Fig. 5). We observed the highest levels of

^{15}N incorporation into glutamate and aspartate, precursors to threonine, in the plasma and liver (Fig. 5). We also saw that the highest levels of ^{15}N incorporation into threonine occur in the small intestine, plasma and liver (Fig. 5). The small intestine serving as the site for threonine synthesis via ^{15}N-aspartate is supported by previous studies indicating that threonine synthesis in mammals relies on gut microbiota.[42] Sections of the small intestine deliver amino acids to the hepatic portal vein, but our experiments cannot determine specific exchanges in the gut-liver axis. Important to note is that many microbial processes are still dependent on NEAA substrate availability, suggesting that metabolic activity of multiple tissues could play supporting roles in free nitrogen recycling for these metabolic pathways in hibernation.[42]

Glutamate and glutamine, along with ATP, are also known nitrogen donors during histidine synthesis.[43] ^{15}N Incorporation into histidine was observed in plasma (1.4±0.3%), liver (0.2±0.6%) and lung (2.1±0.7%) (Fig. 5). We propose ^{15}N glutamine or ^{15}N glutamate are likely sources of ^{15}N histidine via microbial synthesis; we did not observe ^{15}N incorporation into ATP. Given ATP's labile nature, however, lack of detection cannot rule out potential incorporation of ^{15}N into ATP and lack of detection may be attributable to technical limitations. Interestingly, ^{15}N histidine mainly appears in lung and plasma and not small intestine (Fig. 5). Most microbial EAA studies focus on the ileum.[42,44] One explanation for our lack of ^{15}N histidine labeling could be because we did not distinguish between the jejunum and the ileum raising the possibility that our tissue sampling protocol missed a site of small intestine histidine synthesis. The unexpected lung ^{15}N incorporation into histidine parallels the overall broad ^{15}N incorporation into multiple metabolites in lung (Fig. 4). This either suggests lung is an important tissue for nitrogen homeostasis in hibernation or that amino acids carrying recycled nitrogen are important for protein synthesis in lung tissue. While known to play a role in amino acid metabolism, lung metabolism in hibernation is a sparsely investigated field to the best of our knowledge. The high amount of ^{15}N incorporation into histidine and other amino acids in lung suggest that further exploration is worthwhile.

^{15}N Incorporated into glutamine and glutamate also showed evidence of transfer into 5-oxoproline through the gamma-glutamyl cycle. We observed incorporation of ^{15}N into glutamine in plasma (14.1±3.5%), liver (15.1±3.9%), kidney (10.9±4.0%), skeletal muscle (1.9±0.4%), small intestine (3.0±1.6%), and lung (8.4±2.9%) (Fig. 5) and incorporation of ^{15}N into 5-oxoproline in plasma (6.4 ±1.4%), liver (9.0±2.2%), kidney (5.3±1.5%), skeletal muscle (0.4±0.1%), small intestine (1.3±0.4%) and lung (2.7±0.7%) (Fig. 5). Our data is supported by previous findings of significantly increased gamma-glutamylated amino acids during arousal from torpor, showing an active γ-GT (gamma-glutamyltransferase) system, and strong upregulation of antioxidant systems in hibernation.[23,45]

In support of this pathway, data additionally shows that the absolute concentrations of naturally occurring ^{14}N-5-oxoproline significantly correlate with ^{14}N-glutamine and ^{14}N-glutamate levels (Supp. Tables 1a and 1b). We were surprised by the high abundance of naturally occurring ^{14}N 5-oxoproline in plasma (393.34±33.42 μM), liver (6.93±0.76 μM), kidney (3.72±0.39 μM), skeletal muscle (11.15±3.78 μM), small intestine (1.35±0.16 μM) and lung (2.33±0.21 μM) (Supp. Table 1a). Although 5-oxoproline is a common metabolite

across different life forms, in humans increases in 5-oxoproline are documented in pathologies.[46–48] The gamma-glutamyl enzymes are present in most tissues and essential for glutathione function. Previous studies indicate that glutathione can act as a reserve for glutamate with some hypothesizing 5-oxoproline could do the same and that γ-GT is an alternative amino acid transport system.[49–51] Given the elevated absolute concentration of 5-oxoproline in all tissues and its correlation to glutamine and glutamate, 5-oxoproline may represent a substantial pool for nitrogen sequestration in hibernation which could further support antioxidant function and amino acid pools.

Ketoacids increase during natural arousal from torpor

During torpor, WBP of branched chain ketoacids and metabolites (ketoisocaproic acid (KIC), ketoisovalerate acid (KIV), keto-beta-methylvalerate (KMV) and beta-hydroxy-beta-methylbutyrate (HMB)) are suppressed (Fig. 6a, $p<0.002$, WBP torpor vs. WBP summer euthermic, paired two-tailed t-test, n=5). Although it was beyond the scope of this study to capture WBP of these ketoacids during arousal, we next asked if the circulating levels of KIC and KIV and their ketone substrate (acetoacetate) increased in natural arousal from torpor to support nitrogen recycling. As arousal progresses, KIC, KIV and acetoacetate increase as T_b increases (Fig. 6b, $p<0.001$, repeated ANOVA, n=6). Interestingly, in AGS cecal content, branched chain fatty acids are higher in arousal compared to summer and torpor and acetate is higher during hibernation, suggesting microbial metabolism may support production of BCAA ketoacids from branched chain fatty acids.[52] At 16°C leucine/isoleucine decreases, potentially indicating an uptake into tissues (Fig. 6b, $p<0.001$, repeated ANOVA, n=6). Pathway enrichment analysis identified amino acid metabolism and BCAA biosynthesis as metabolically significant over the course of arousal (Fig. 7, $p<0.001$ ANOVA, FDR-adjusted p value). The increase of BCAA ketoacids and their ketone parent (acetoacetate) in natural arousal from torpor supports nitrogen recycling by increasing availability of substrate for BCAA synthesis.

Discussion:

The source and fate of free nitrogen during hibernation has until now been poorly understood. During interbout arousal, free nitrogen is recycled and buffered by transamination reactions into glutamate and glutamine and then incorporated into essential amino acids (EAA), non-essential amino acids (NEAAs) and the gamma-glutamyl intermediate 5-oxoproline. Nitrogen recycling has been proposed for decades as a potential mechanism of nitrogen homeostasis in hibernation. Our work, for the first time, demonstrates metabolic pathways facilitating nitrogen recycling *in vivo* and shows that free nitrogen is incorporated into metabolites. These metabolites may support protein synthesis and antioxidant capacity during arousal from torpor. Previous studies hypothesized that free EAAs, which support skeletal muscle and whole body protein synthesis, originate from collagen breakdown in labile protein sources during hibernation.[4,18,35,36] We show that, although suppressed, skeletal muscle breakdown is greater than collagen breakdown in torpor suggesting that skeletal muscle breakdown contributes to circulating amino acids and increased nitrogen load in torpor to a greater degree than collagen breakdown.

Nitrogen recycling has been proposed for decades as a potential mechanism of metabolic homeostasis and physiological support in hibernation.[6,7,16] Our work demonstrates unequivocally nitrogen recycling and de novo EAA synthesis and highlights pathways that support this metabolic mechanism. Our results suggest that inter-organ cooperation in metabolism supports synthesis of metabolites. These metabolites are essential components of tissue protein synthesis and have anabolic signaling properties and other physiological roles.[27] Our findings highlighting recycling of nitrogen into NEAAs to support EAA synthesis expand on previous models predicting increased NEAA synthesis in hibernating bears.[34] ^{15}N Incorporation into 5-oxoproline also represents a novel pathway for recycling and buffering free nitrogen, while supporting previous studies suggesting 5-oxoproline and glutathione could act as pools for glutamate.[49,50] In the greater context, antioxidants are known to be upregulated in hibernation and protect skeletal muscle from injury.[45,53] Sequestration of nitrogen into the gamma-glutamyl cycle would support glutathione synthesis and antioxidant defense. Hibernators preserve their muscle mass and functionality despite extreme inactivity and prolonged fasting.[2,4,18,54–57] While previous research has debated the extent of muscle preservation and the mechanisms responsible, we have documented the retention of lean tissue mass in AGS using dual energy x-ray absorptiometry during prolonged inactivity or forced disuse (neurectomy).[2] Similarly, preservation of lean tissue mass determined by naturally occurring tissue nitrogen isotope ratios (δ15N) was noted in AGS housed throughout the hibernation season at mild ambient temperature of 2°C.[7] By contrast, when housed at a colder ambient temperature (−10°C) such as experienced in the wild, there was a reduction in lean tissue mass in proportion to the total number of days of the hibernation season.[7,9] Thus, milder ambient temperatures reveal a resistance to disuse atrophy not seen in non-hibernating species.[2,55,56,58] Our analysis of liver and small intestine support Lee's interpretation of protein synthesis in these tissues during the hibernation season and suggest protein synthesis may occur in tissues such as lung, kidney and skeletal muscle to a lesser extent.

Our findings also support previous gene expression studies in AGS muscle that indicate protein anabolism persists throughout the hibernation season while proteasome, autophagy and atrogene gene expression are not changed or are downregulated.[4,59] Metabolic pathways facilitating ^{15}N recycling could directly support muscle protein synthesis during interbout arousal.[1,4,18,55,58,60]

While our data clearly shows enrichment of ^{15}N in these key energy metabolites, there are some important caveats to consider. We observed lower ^{15}N incorporation into EAA in skeletal muscle than in kidney, lung or liver. One reason for this could be regional temperature differences during rewarming.[61,62] Tissues were collected 2 hours after IV bolus infusion during arousal; the head and thoracic region of the body warms more quickly than distal regions partially due to proximity of brown adipose tissue deposits and distal vasoconstriction.[61] Further, in AGS arousal, blood flow to the extremities significantly lags behind brain and organ blood flow, meaning that metabolic exchanges with circulation occur more quickly for the brain and visceral tissues than for the quadriceps.[62] If experiments had taken place during full arousal (T_b>34°C) for a longer duration, we might have seen higher incorporation of labeled ^{15}N in all tissues and peripheral skeletal muscle that lags in rewarming.

Indeed, we observed temperature dependent incorporation of ^{15}N into amino acids in several tissues. We designed the ^{15}N ammonium acetate infusion to standardize the time between infusion and sample collection. As a result, we collected tissues across a wide range of T_b due to variation in rates of rewarming. This allowed us to define linear relationships between T_b and degree of ^{15}N incorporation in some tissues. The novel insight from this approach is that many of these mechanisms incorporate ^{15}N into metabolites at temperatures as low as 5°C (albeit, at reduced rates). Ketoacids, however, only increase as temperatures reach 16°C. Therefore, ^{15}N incorporation into leucine/isoleucine and large-scale synthesis of EAA may be temperature dependent (Extended Fig. 2). This is consistent with previous findings that translation has a temperature threshold of 18°C in 13-lined ground squirrels.[63]

The scope of this study did not include measures of 3-MH or hPRO WBP rates during arousal. Arousal from torpor has a period of intense shivering and rapid physiological and metabolic changes. While we saw high rates of 3-MH production in deep torpor, it remains unknown if this trend continues or reverses during the arousal period. Additional metabolic flux analysis was not possible during interbout arousal because isotope from one infusion could have confounded an additional pulse study in the same animal during the hibernation season. While most of the total mammalian 3-MH pools exist in skeletal muscle, 3-MH is also present in actin in all cell types. Prior studies have pointed out that increased rates of 3-MH production could be partially caused by high rates of turnover in these actin pools.[22] We interpret 3-MH as a marker of skeletal protein degradation rather than actin turnover due to the direct correlation of 3-MH to catabolism in leg muscle.[20]

In summary, our results support a model of skeletal muscle breakdown and nitrogen accumulation in torpor with ammonia salvage pathways funneled away from the urea cycle and into, EAA, NEAA, and the gamma-glutamyl pathway during arousal. Many of these amino acids are direct precursors and signaling metabolites necessary for protein synthesis.

This work has translational significance as a model of metabolic resilience during extreme inactivity and nutrient deficiency. AGS utilize specific metabolic mechanisms to sustain nitrogen stores and deliver critical amino acids which are essential for protein synthesis and organ function. In the absence of mechanical loading, the maintenance oriented mechanisms responsible for the preservation of musculoskeletal system and physical function in hibernation are highly relevant to our understanding of clinical perturbations such as sarcopenia, cachexia and even spaceflight.[64] Now recognized as therapeutic targets for accelerated muscle atrophy in humans, these protective mechanisms may also be positively influenced by the preservation of molecular mechanisms such as miRNAs that dampen the influence of myostatin and ubiquitin ligase in hibernating species.[65,66] Future work should incorporate these active metabolic mechanisms with known molecular mechanisms that augment protein maintenance in hibernation to find novel therapeutic targets.

Methods:

Trapping:

Arctic Ground Squirrels (AGS, *Urocitellus parryii)* were trapped in early July in the northern foothills of the Brooks Range, Alaska, 40 miles south of Toolik Field Station (68°38 N,

149°38 W; elevation 809 m) and were transported to Fairbanks, Alaska under permit by the Alaska Department of Fish and Game (permit numbers 18-111 and 17-156).

Ethic Overview:

All procedures were performed in accordance with University of Alaska Fairbanks Institutional Animal Care and use Committee (IACUC, protocols 491809 and 996835).

Husbandry:

AGS were housed in ambient temperature (T_a) between 16-18°C at 16:8-hour light/dark cycle until August 15th, when they were moved to cold chambers with T_a of 2°C at a 4:20 hour light/dark cycle. Animals were fed Mazuri Rodent chow (#5663 Mazuri, PMI Nutrition International, Richmond, IN, USA) and provided water during the euthermic period. Animals were housed individually in 12”×19”×12” stainless steel wire mesh hanging cages with cotton nests over ammonia absorbing corn cob litter. Once animals exhibited robust hibernation behavior, food was withdrawn; animals were placed in polycarbonate cages (8.5”×17”×8.5”) with shavings, cotton bedding and gel hydration packets. Polycarbonate cages were placed on receivers linked to a data collection system for core body temperature (Data Sciences International, St. Paul, MN, USA).

Surgery:

AGS were instrumented with chronic femoral arterial and venous cannulas (3 Fr cannula, Instech Laboratories Inc, Plymouth Meeting, PA, USA) and either TA-F40 or CTA-F40 core body temperature loggers (Data Sciences International, St. Paul, MN, USA) in July and August. Cannulae patency was maintained with a heparin/glycerol locking solution (1:1).

Chemicals:

A mixture of amino acid isotopes (Cambridge Isotope Laboratories, Woburn, MA USA) was compounded professionally in a compounding pharmacy (Temple, TX). For specific mixture composition see Fig. 1. ^{15}N Ammonium acetate (98%, Sigma-Aldrich, St. Louis, MO) was diluted in saline and sterilized by 0.2 μm filtration.

Definition of hibernation state:

Torpor is defined as the time when core body temperature is below 4°C. The first day of torpor is defined by a T_b of 4°C reached after a period of stable euthermic T_b (34-36°C). Entrance into torpor is defined during the period of decreasing T_b when T_b is within 10-11°C. We recorded body weight during the euthermic period preceding experiments.

Deep Torpor and Summer: Design for Whole Body Production Measurement with Pulse Isotope Infusions:

We administered mixed pulse isotope infusions (Fig. 1) in February during deep torpor on the third day of a torpor bout (Fig. 1, female n=5, male n=4). Infusions did not affect torpor (torpid T_b did not vary more than 0.12°C during experimental procedures). We flushed AGS cannula with sterile saline on the first and second day of torpor to habituate animals to cannula handling. If flushing induced arousal, animals were excluded from experimental

procedures. Experiments began in the morning on the third day of torpor. Heparinized saline locking solution was removed and blood was sampled from the cannula prior to pulse infusion of a mixed amino acid isotope cocktail (0 hour). Blood was then sampled at precisely 10 min, 20 min, 30 min, 1 hour, 2 hour, 3 hour, 4 hour, 12 hour and 24 hour post infusion. Control experiments were repeated in summer (June) with the same animals under post-absorptive conditions after an overnight fast (female n=2, male n=3, cannuale patency was lost on a few animals over the winter season resulting in the decreased summer sample size). Blood sampled during the summer season was sampled immediately prior to infusion (0 hour), and at 5 min, 10 min, 15 min, 20 min, 30 min, 1 hour, 1.5 hour and 2 hour. Blood was sampled via the arterial line and collected into a 1cc syringe via a pin port and immediately transferred to a non-heparinized micro-hematocrit tube (Kimble) and sealed with putty. Blood was centrifuged for 2 min at 4°C and plasma was immediately placed on dry ice. Samples were transferred to a −80°C freezer and stored until shipped to Texas A&M for analysis. Core body temperature (Tb) was recorded at 10-minute intervals throughout the hibernation season.

Deep Torpor and Summer Quantification of rates of Whole Body Metabolite Production:

Deep torpor and summer metabolites and enrichments of tracers were measured batch-wise by stable tracer-dilution LC-MS/MS as previously described.[19] While amino acid and metabolite production in vivo is often measured by primed-constant infusions of stable isotope tracers, torpor and arousal from torpor are non-steady-state physiological conditions with unknown metabolite production rates and metabolite pool sizes.[19,67] Pulse isotope tracer methodology is the preferred technique to measure non-steady state conditions by measuring decay curves with noncompartmental modeling.[19,67,68] In brief, deproteinized plasma supernatants were diluted in reagents required for a 9-fluorenylmethoxycarbonyl (Fmoc) reaction. Reactions were stopped after 15 minutes. We injected 0.2–1.7 μL into the 24 μl/min pumped flow (microLC 200, Eksigent, part of AB Sciex) of 73:23:4 water-acetonitrile-isopropanol containing 11 mM ammonium acetate, onto a 100 × 0.5 mm column packed by Eksigent with 2.7 μm 90 Å HALO C18 fused-core silica beads (Advanced Materials Technology). Fmoc-amino acids eluted over 3.2 min; bis-Fmoc-amino acids (ornithine, and tyrosine) eluted by 4.5 min. Ions were conveyed by heated electrospray (−3.8 kV IS; 150°C TEM; 14 GAS1; 25 GAS2) to a 5500 QTRAP (Sciex) for multiple reaction monitoring (MRM) of the loss of the Fmoc moiety or moieties, regenerating the amino acid anion. Collision energy (CE) was de-optimized as needed for analytes that would otherwise risk detector saturation. Peaks were automatically identified and integrated by the SignalFinder1 algorithm in MultiQuant v. 3.0 (Sciex) and integrations were inspected. Manual reintegration (redrawing of baselines and peak boundaries) was disallowed, but manual reidentification was allowed as needed. Peak areas were exported to Excel for calculation of area ratios for 1) concentration measurements using a tracer for the internal standard and 2) enrichment measurements of an exogenous tracer (or tracer metabolite) to the corresponding amino acid. Area ratios of calibrators were regressed against calibrator known tracer-to-tracee ratios (TTR) by ordinary least squares (Prism 8, GraphPad). By reverse prediction, each plasma sample area ratio was converted to a TTR. Previous experiments have documented that the pulse isotope infusion does not affect the tracee concentration.[19]

Calculations of Whole Body Production:

The decay of TTR over time was normalized with body weight and amount of administered tracer (Prism 8, Graphpad). Decay of TTR amino acid isotopes were fitted to the equation y=a*exp(−k1*x)+b*exp(−k2*x), where k1 and k2 are decay rate constants of tracer and tracee, and area under the curve (AUC) was calculated from the integral of the two exponential curves.[68] Rate of appearance (Ra) for each amino acid is calculated by: dose of metabolite in the pulse infusion/decay of metabolite tracer (AUC). Whole body rate of appearance (Ra) of amino acids is a proxy for whole body production (WBP).

Metabolomic Deep Torpor Profiling Experimental Procedure:

Animals were habituated to cannula flushing with sterile saline. Plasma was sampled from naïve hibernating AGS without disturbing hibernation over a full torpor bout (Fig. 1, female n=5, male n=4). Sampling occurred during entrance to torpor (T_b 11-12°C) and sequentially through a full torpor bout. Six animals were also sampled through a natural arousal at four time points during re-warming: 2.5°C, 4°C, 16°C and 35°C. A typical torpor bout is a 14 to 20-day period while a typical arousal is a 12-24 hour period, though timing varies depending on ambient temperature and season.[10] Relative abundance of metabolites was normalized to entrance levels (T_b 11-12°C). Duration of torpor was expressed as a percentage of the total length of the torpor bout in days.

Longitudinal Global Metabolomic Quantification:

Plasma samples (20 μl) were extracted using ice cold methanol:acetonitrile:water (5:3:2) at 1:25 dilution as described.[69] Extracts were analyzed on a Thermo Vanquish ultra-high performance liquid chromatograph (UHPLC) coupled online to a Thermo Q Exactive mass spectrometer using a 5 min C18 gradient method in positive and negative modes as described previously.[24,70] Peak picking and metabolite assignment were performed using Maven (Princeton University) against the KEGG database (https://www.genome.jp/kegg), [71,72] confirmed against chemical formula determination from isotopic patterns and accurate mass, and validated against experimental retention times for >650 standard compounds (Sigma Aldrich; MLSMS, IROATech, Bolton, MA, USA).[73]

Compartmental Nitrogen (^{15}N) Flux in Arousal from Torpor Experimental Procedure:

^{15}N-Ammonium acetate experiments occurred on the third day of a torpor bout in February in a separate animal group from previous tracer studies. Arousal was induced by handling between 0730 and 0830 in the morning. Importantly, while re-warming rates vary slightly between handling-induced vs. spontaneous arousal, inducing arousal was not expected to influence outcome of the study. As Williams et al. (2011) has noted, differences in metabolic energetic demand on AGS (in a different circumstance, hibernating at two different temperatures), did not alter transcript levels in major metabolic tissues such as BAT and liver.[74] A ^{15}N ammonium acetate venous bolus of either 72 mg/kg (female n=3, male n=3) or 360 mg/kg (female n=3, male n=2) at a volume of 1 ml/kg was infused 1.5 hours after inducing arousal (Fig. 1). Blood was sampled two hours post infusion under a surgical plane of anesthesia (induced at 5% isoflurane with 100% medical grade oxygen). Animals were euthanized (by decapitation) directly afterwards and tissues were rapidly sampled and frozen

on dry ice. Because the time between bolus and sample collection was standardized to two hours post infusion, rectal temperature of AGS taken at time of tissue collection varied from 4.9-24.4°C. Tissue samples included liver (left lobe), kidney (cortex), skeletal muscle (right quadriceps femoris), lung (right), plasma, and small intestine (cleaned from mesentery). Tissue samples were extracted in ice-cold lysis/extraction buffer (described above) at a concentration of 15 mg/mL in the presence of glass beads. Samples were agitated via bead beater for 3 min at 4°C then vortexed for 30 minutes and centrifuged at 18,200 g for 10 minutes at 4°C. Plasma samples (20 μl) were extracted as described above.

^{15}N Tracer Metabolite Quantification:

Plasma and tissue extracts were analyzed by UHPLC-MS as described above (see longitudinal metabolomics sampling). Animals in this experiment had no previous tracer infusions. Major metabolites for nitrogen metabolism were inspected for ^{15}N incorporation including purine, amino acid, creatine, spermidine, urea cycle and 5-oxoproline metabolism. Isotopologue distributions were corrected for natural abundance and results were plotted in GraphPad Prism 8.0.

Statistical Analysis:

Results were expressed as mean +/− standard error of the mean (S.E.M). Significance of difference was assessed by repeated measures ANOVA, post hoc LSD and two-tailed student's t-test as specified using SPSS (version 25, IBM SPSS Statistics, Armornk, NY). Measurements that violated sphericity were reported with greenhouse-geisser (G-G) corrections and t-tests that violated Levene's test for equality were performed without assuming equal variances. Pathway enrichment analysis was performed using MetaboAnalyst 4.0. GraphPad Prism (version 8, GraphPad Software Inc., La Jolla, CA) was used for graphic presentation. Treatment groups were matched for sex and hibernation phase timing. Treatment was not blinded and no data was excluded.

Sample size was determined by availability of wild-caught animals, but guided by a priori power analysis based on published literature.[11] A priori power analysis (G*Power software) was performed to estimate sample size needed to yield 80% power with 0.05 α error probability for a two tailed t-test. A priori power analysis indicated that a sample size of eight animals with an expected difference in means of 0.20 and standard deviations of 0.15 and 0.11 (based on metabolite data taken from thirteen lined ground squirrel late torpor versus entrance) would have power of 0.81. In our studies, a sample size of nine was chosen to account for attrition.

Extended Data

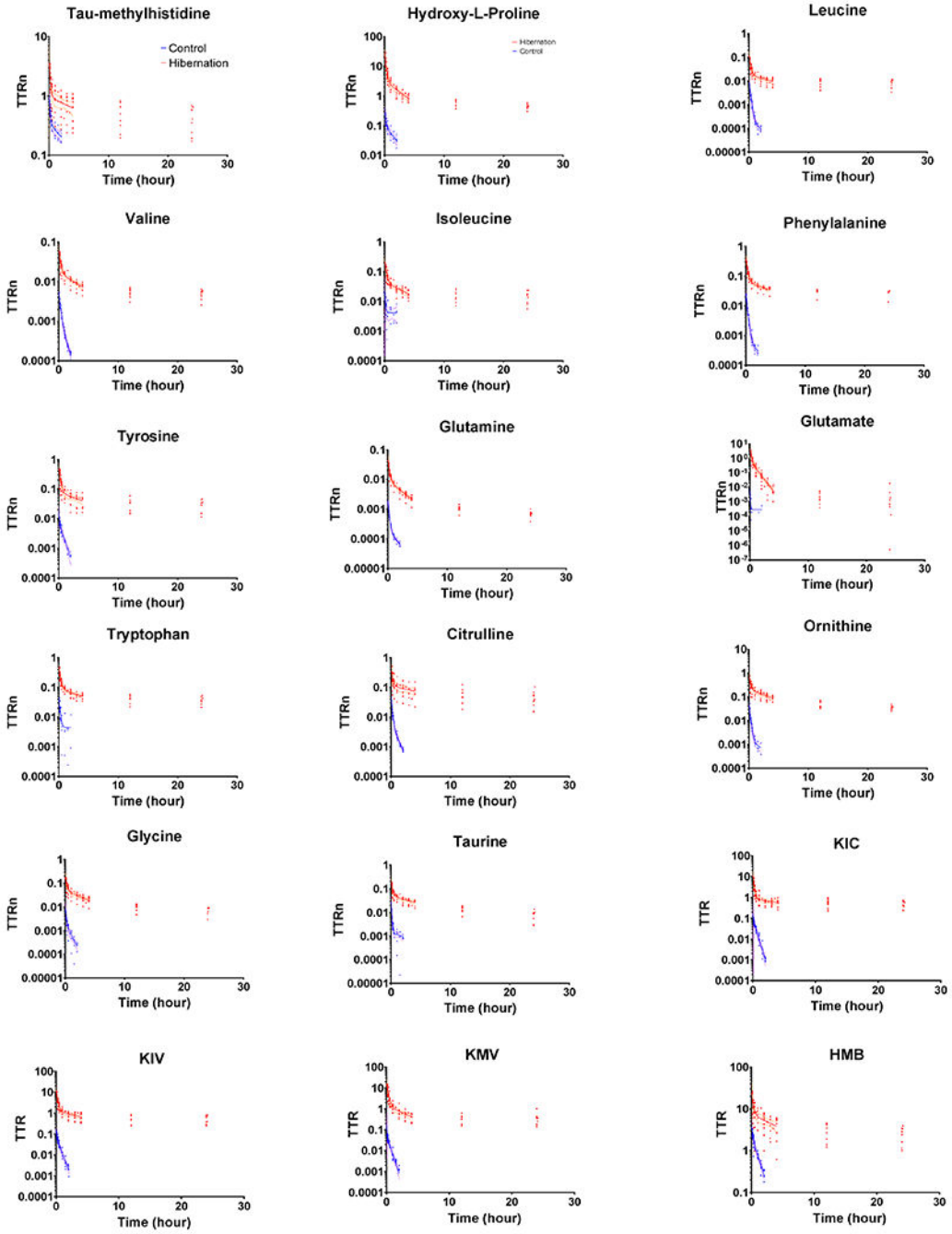

Extended Figure 1.

Tracer to tracee ratio (TTR) decay curves show slow decay in torpor (red, n=9) compared to summer euthermic AGS (blue, n=5). Decay of TTR amino acid isotopes were fitted to the equation y=a*exp(−k1*×)+b*exp(−k2*×), and area under the curve (AUC) was calculated from the integral of the two exponential curves. Rate of appearance (Ra) for each amino acid

is calculated by: dose of metabolite in the pulse infusion/AUC. Whole body rate of appearance (Ra) of amino acids is a proxy for whole body production (WBP).

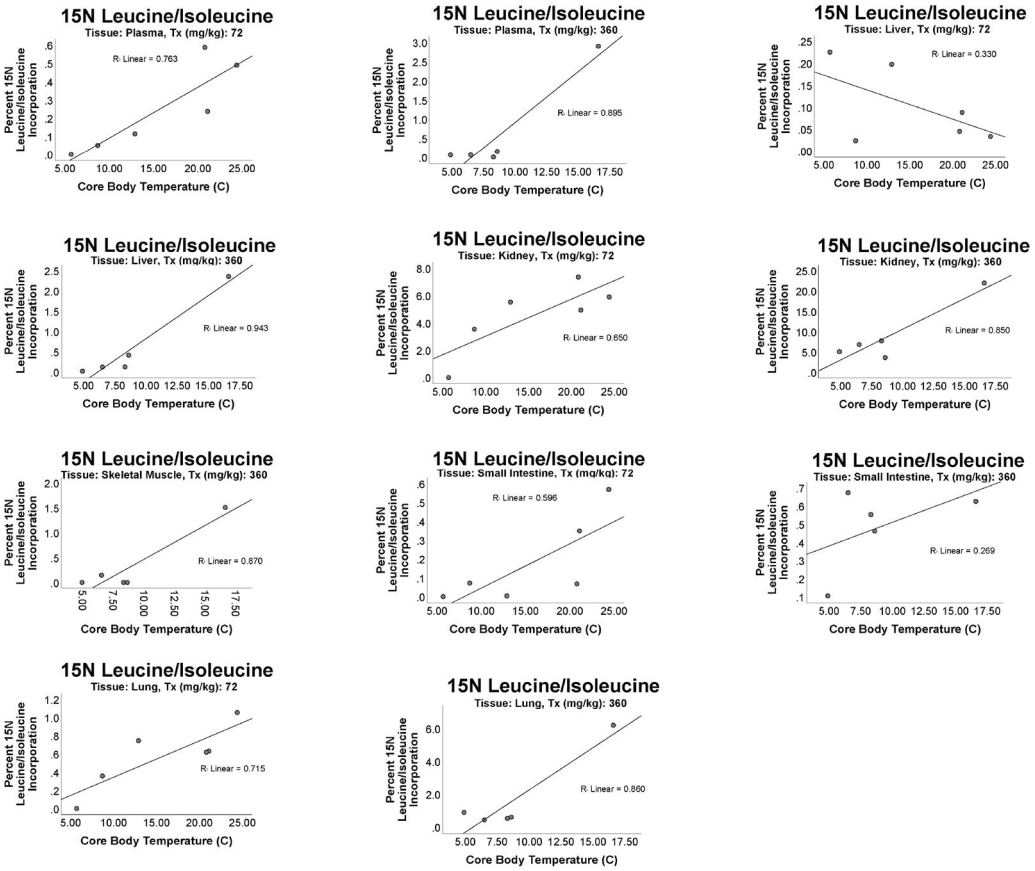

Metabolite	Tx (mg/kg)	Tissue	R Square	Intercept	Slope	F	p value
^{15}N Leucine/Isoleucine	72	Kidney	0.650	4.705	2.397	7.437	0.053
	360	Kidney	0.850*	3.888	0.563	17.018	**0.026**
	72	Liver	0.330	20.676	-49.630	1.973	0.233
	360	Liver	0.943*	6.286	4.432	49.345	**0.006**
	72	Lung	0.715*	5.436	17.903	10.039	**0.034**
	360	Lung	0.860*	6.070	1.675	18.418	**0.023**
	72	Plasma	0.763*	8.849	27.387	12.906	**0.023**
	360	Plasma	0.895*	6.820	3.371	25.505	**0.015**
	360	Skeletal Muscle	0.870*	6.876	6.367	20.043	**0.021**
	72	Small Intestine	0.596	11.122	25.268	5.892	0.072
	360	Small Intestine	0.269	3.968	10.352	1.106	0.37

Extended Figure 2:

Linear regression analysis indicates ^{15}N incorporation into leucine/isoleucine is correlated to core body temperature during arousal from torpor (72 mg/kg ^{15}N ammonium acetate pulse infusion n=6, 360 mg/kg ^{15}N ammonium acetate pulse infusion n=5). In tissues where

nitrogen incorporation was not observed in more than one animal, regression analysis was not preformed.

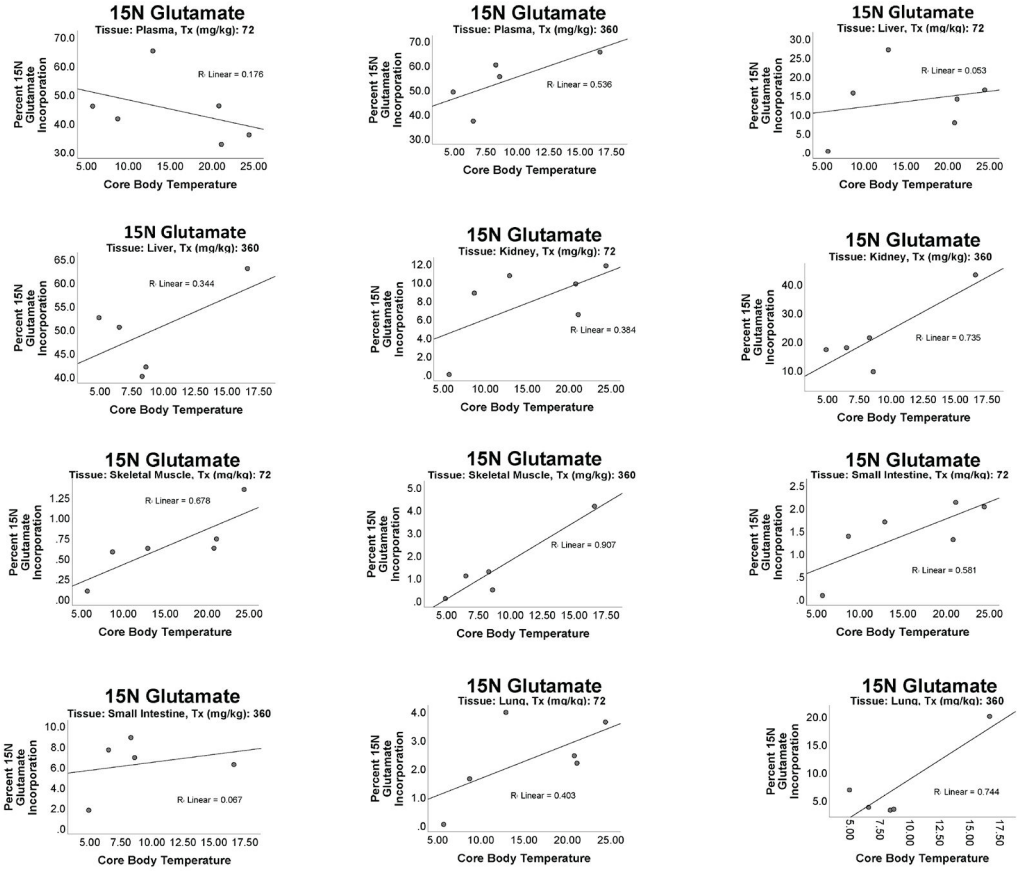

Metabolite	Tx (mg/kg)	Tissue	R Square	Intercept	Slope	F	p value
^{15}N Glutamate	72	Kidney	0.384	6.900	1.097	2.489	0.19
	360	Kidney	0.735	2.318	0.305	8.326	0.063
	72	Liver	0.053	12.965	0.195	0.226	0.659
	360	Liver	0.344	-5.324	0.288	1.571	0.299
	72	Lung	0.403	7.771	3.374	2.703	0.176
	360	Lung	0.744	6.280	0.429	8.718	0.06
	72	Plasma	0.176	28.050	-0.279	0.855	0.407
	360	Plasma	0.536	-7.218	0.303	3.471	0.159
	72	Skeletal Muscle	0.678*	5.169	15.569	8.437	**0.044**
	360	Skeletal Muscle	0.907*	5.175	2.678	29.132	**0.012**
	72	Small Intestine	0.581	4.429	7.780	5.537	0.078
	360	Small Intestine	0.067	6.280	0.429	0.214	0.675

Extended Figure 3:

Linear regression analysis indicates ^{15}N incorporation glutamate in skeletal muscle is correlated to core body temperature during arousal from torpor (72 mg/kg ^{15}N ammonium acetate pulse infusion n=6, 360 mg/kg ^{15}N ammonium acetate pulse infusion n=5). In tissues

where nitrogen incorporation was not observed in more than one animal, regression analysis was not preformed.

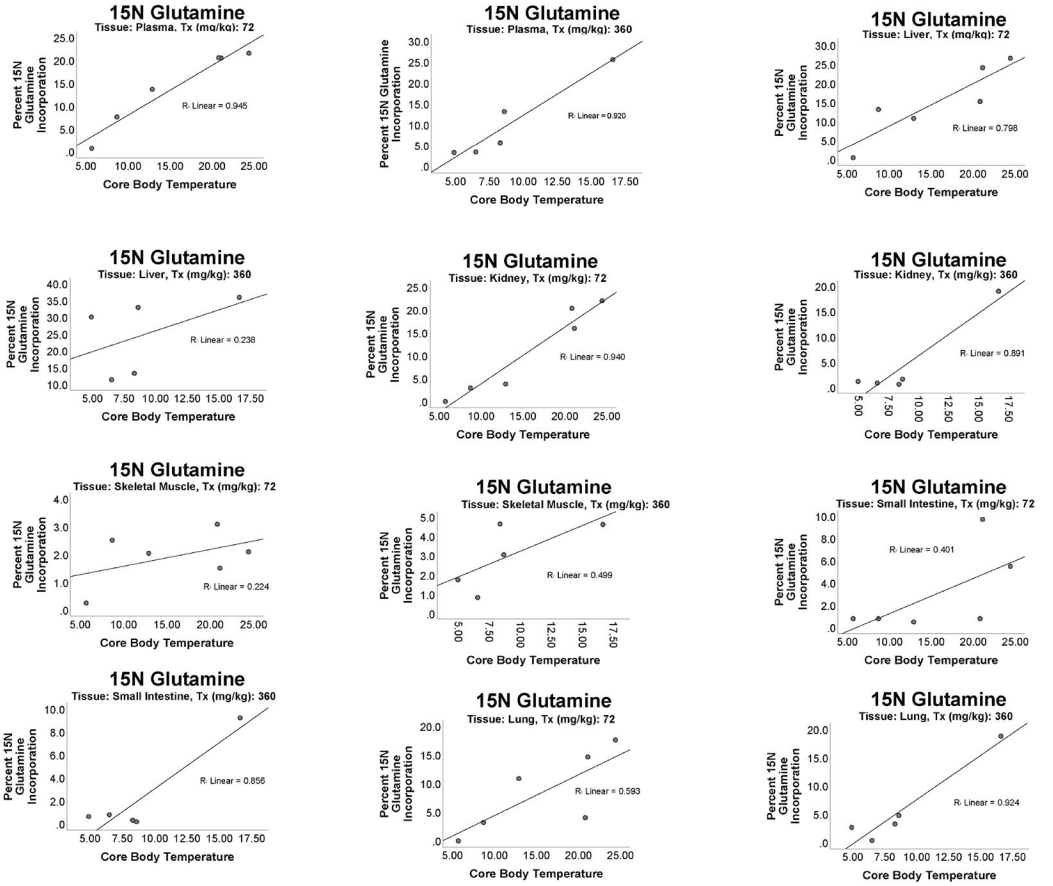

Metabolite	Tx (mg/kg)	Tissue	R Square	Intercept	Slope	F	p value
^{15}N Glutamine	72	Kidney	0.940*	7.377	0.758	62.349	**0.001**
	360	Kidney	0.891*	6.492	0.531	24.538	**0.016**
	72	Liver	0.798*	4.848	0.713	15.759	**0.017**
	360	Liver	0.238	4.246	0.191	0.935	0.405
	72	Lung	0.593	8.608	0.831	5.830	0.073
	360	Lung	0.924*	5.442	0.591	36.419	**0.009**
	72	Plasma	0.945*	3.333	0.868	69.079	**0.001**
	360	Plasma	0.920*	4.318	0.456	34.578	**0.01**
	72	Skeletal Muscle	0.224	8.494	3.701	1.157	0.343
	360	Skeletal Muscle	0.499	3.391	1.875	2.984	0.183
	72	Small Intestine	0.401	11.788	1.262	2.682	0.177
	360	Small Intestine	0.856*	6.602	1.065	17.895	**0.024**

Extended Figure 4:

Linear regression analysis indicates ^{15}N incorporation into glutamine is correlated to core body temperature during arousal from torpor in kidney, plasma and liver (72 mg/kg ^{15}N ammonium acetate pulse infusion n=6, 360 mg/kg ^{15}N ammonium acetate pulse infusion

n=5). In tissues where nitrogen incorporation was not observed in more than one animal, regression analysis was not preformed.

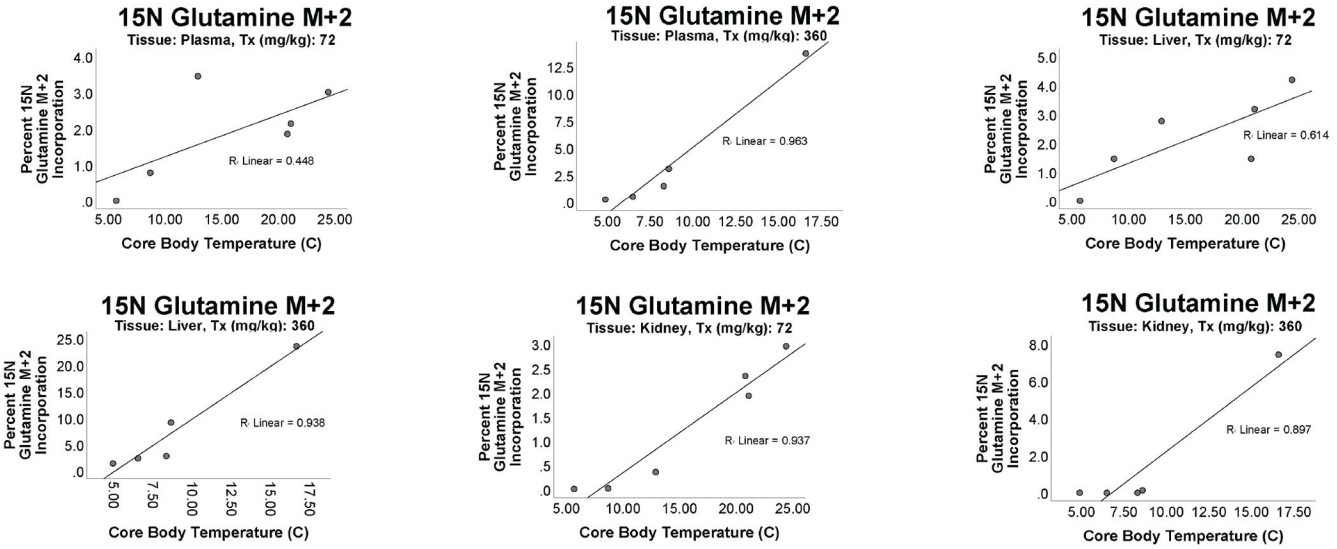

Metabolite	Tx (mg/kg)	Tissue	R Square	Intercept	Slope	F	p value
^{15}N Glutamine M+2	72	Kidney	0.937*	8.385	5.660	59.641	**0.002**
	360	Kidney	0.897*	7.023	1.291	26.111	**0.015**
	72	Liver	0.614	6.937	3.964	6.368	0.065
	360	Liver	0.938*	5.260	0.471	45.773	**0.007**
	72	Plasma	0.448	8.320	3.868	3.251	0.146
	360	Plasma	0.963*	5.965	0.787	78.997	**0.003**

Extended Figure 5:

Linear regression analysis indicates ^{15}N incorporation into Glutamine M+2 is correlated to core body temperature in kidney and liver during arousal from torpor (72 mg/kg ^{15}N ammonium acetate pulse infusion n=6, 360 mg/kg ^{15}N ammonium acetate pulse infusion n=5). In tissues where nitrogen incorporation was not observed in more than one animal, regression analysis was not preformed.

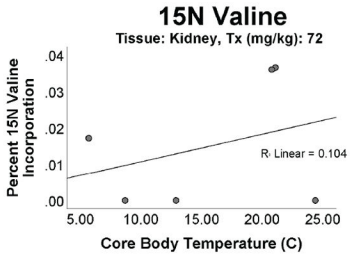

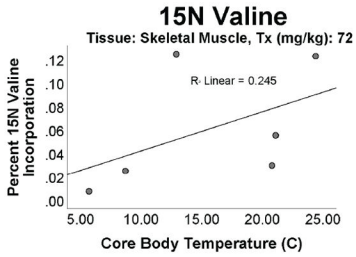

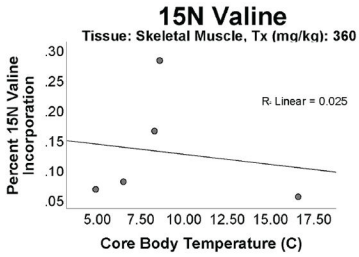

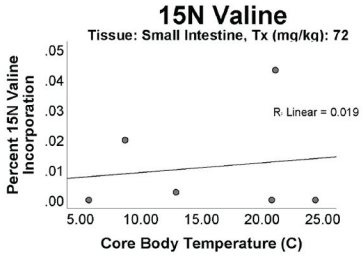

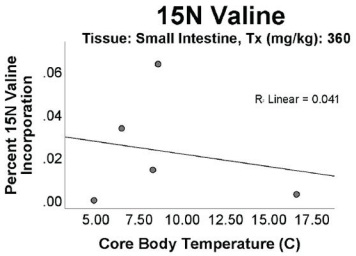

Metabolite	Tx (mg/kg)	Tissue	R Square	Intercept	Slope	F	p value
^{15}N Valine	72	Kidney	0.104	13.544	137.479	0.465	0.533
	72	Skeletal Muscle	0.245	11.096	73.697	1.300	0.318
	360	Skeletal Muscle	0.025	9.960	-7.498	0.078	0.799
	72	Small Intestine	0.019	14.942	60.137	0.079	0.792
	360	Small Intestine	0.041	9.769	-34.668	0.127	0.745

Extended Figure 6:

Linear regression in analysis indicates ^{15}N incorporation into valine cannot be verified to rely on core body temperature during arousal from torpor. In tissues where nitrogen incorporation was not observed in more than one animal, regression analysis was not preformed

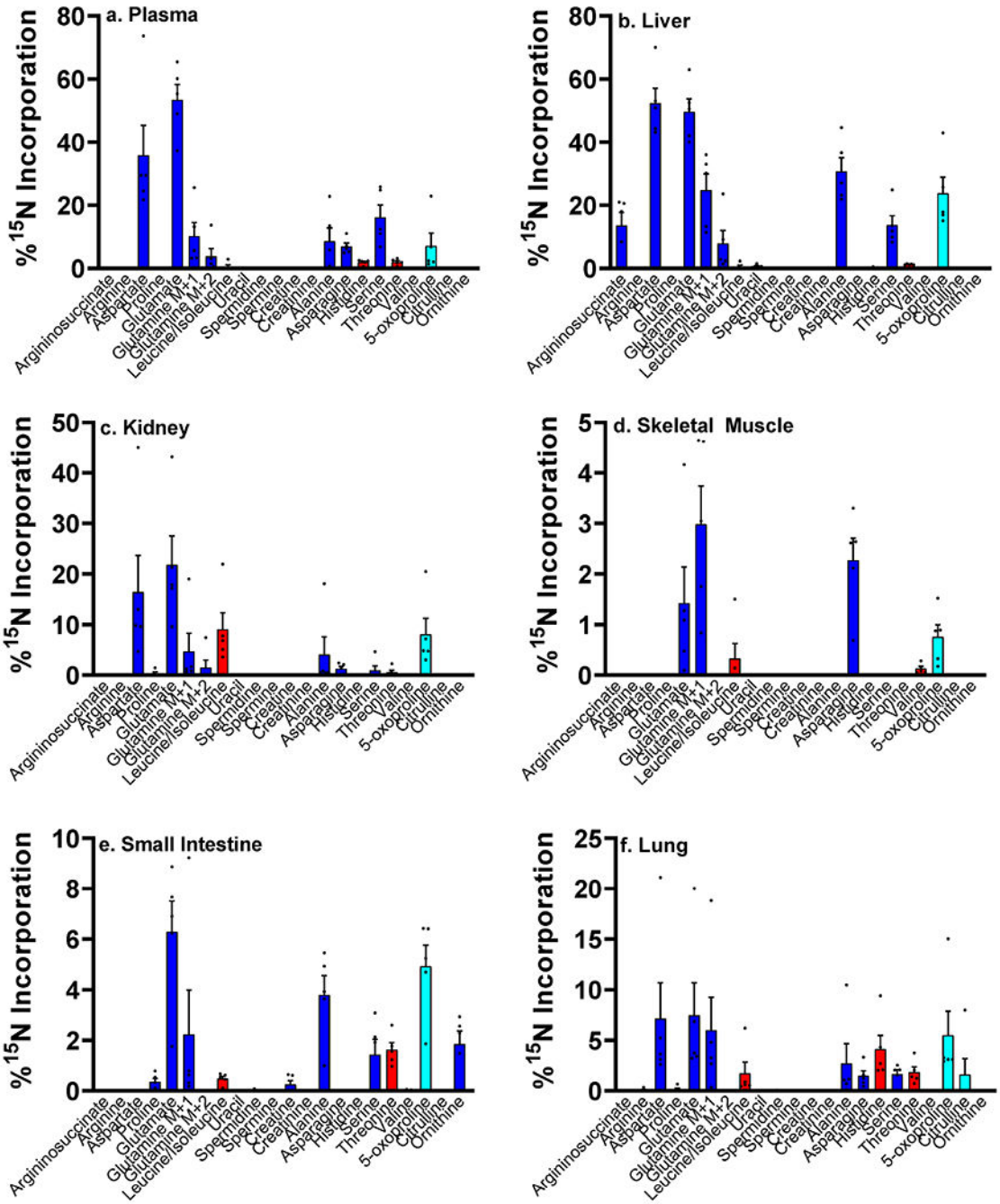

Extended Figure 7.

Free ^{15}N ammonia is recycled into nonessential amino acids (blue), essential amino acids (red) and 5-oxoproline (turquoise) during arousal from torpor (360 mg/kg ^{15}N ammonium acetate pulse infusion, n=5, mean ±SEM). Percent ^{15}N incorporation calculated as: (^{15}N metabolite peak area/(^{15}N metabolite peak area + ^{14}N metabolite peak area))*100 following natural abundance correction.

Supplementary Material

Refer to Web version on PubMed Central for supplementary material.

Acknowledgements

We thank Chris Terzi and Carla Willetto for their veterinary assistance and Hoshi Sugiura, Monica Mikes and Melanie Roed for assistance with animal husbandry. We also thank Jack Reakoff for generous use of his cabin while trapping and Jeanette Moore for thoughtful and wise advice.

Funding: Research reported in this publication was supported by NSF IOS 1258179 and by Institutional Development Awards (IDeA) from the National Institute of General Medical Sciences of the National Institutes of Health under grant numbers 2P20GM103395 and P20GM130443. AD was supported by funds from the Boettcher Foundation Webb-Waring Early Career Award 2017, the National Institute of General Medical Sciences (RM1GM131968) and the National Heart, Lung and Blood Institute (R01HL146442 and R01HL148151). The content is solely the responsibility of the authors and does not necessarily represent the official views of the National Institutes of Health.

References

1. Carey HV, Andrews MT & Martin SL Mammalian hibernation: cellular and molecular responses to depressed metabolism and low temperature. Physiol Rev 83, 1153–1181, doi:10.1152/physrev.00008.2003 (2003). [PubMed: 14506303]
2. Bogren LK et al. The effects of hibernation and forced disuse (neurectomy) on bone properties in arctic ground squirrels. Physiol Rep 4, doi:10.14814/phy2.12771 (2016).
3. Barnes BM Freeze avoidance in a mammal: body temperatures below 0 degree C in an Arctic hibernator. Science 244, 1593–1595 (1989). [PubMed: 2740905]
4. Fedorov VB et al. Comparative functional genomics of adaptation to muscular disuse in hibernating mammals. Mol Ecol 23, 5524–5537, doi:10.1111/mec.12963 (2014). [PubMed: 25314618]
5. Harlow HJ, Lohuis T, Beck TD & Iaizzo PA Muscle strength in overwintering bears. Nature 409, 997, doi:10.1038/35059165 (2001). [PubMed: 11234052]
6. Barboza PS, Farley SD & Robbins CT Whole-body urea cycling and protein turnover during hyperphagia and dormancy in growing bears (Ursus americanus and U. arctos). Canadian Journal of Zoology 75, 2129–2136, doi:10.1139/z97-848 (1997).
7. Lee TN, Buck CL, Barnes BM & O'Brien DM A test of alternative models for increased tissue nitrogen isotope ratios during fasting in hibernating arctic ground squirrels. J Exp Biol 215, 3354–3361, doi:10.1242/jeb.068528 (2012). [PubMed: 22735347]
8. Steffen JM, Rigler GL, Moore AK & Riedesel ML Urea recycling in active golden-mantled ground squirrels (Spermophilus lateralis). Am J Physiol 239, R168–173, doi:10.1152/ajpregu.1980.239.1.R168 (1980). [PubMed: 7396033]
9. Buck CL & Barnes BM Effects of ambient temperature on metabolic rate, respiratory quotient, and torpor in an arctic hibernator. Am J Physiol Regul Integr Comp Physiol 279, R255–262, doi:10.1152/ajpregu.2000.279.1.R255 (2000). [PubMed: 10896889]
10. Karpovich SA, Toien O, Buck CL & Barnes BM Energetics of arousal episodes in hibernating arctic ground squirrels. J Comp Physiol B 179, 691–700, doi:10.1007/s00360-009-0350-8 (2009). [PubMed: 19277682]
11. Serkova NJ, Rose JC, Epperson LE, Carey HV & Martin SL Quantitative analysis of liver metabolites in three stages of the circannual hibernation cycle in 13-lined ground squirrels by NMR. Physiol Genomics 31, 15–24, doi:10.1152/physiolgenomics.00028.2007 (2007). [PubMed: 17536023]
12. Emirbekov EZ & Mukailov MI [Ammonia, glutamine and urea concentration in the brain tissue of susliks during winter hibernation]. Biull Eksp Biol Med 69, 64–66 (1970).
13. Cooper AJ & Freed BR Metabolism of [13N]ammonia in rat lung. Neurochem Int 47, 103–118, doi:10.1016/j.neuint.2005.04.013 (2005). [PubMed: 15923062]

14. Brusilow SW & Cooper AJ Encephalopathy in acute liver failure resulting from acetaminophen intoxication: new observations with potential therapy. Crit Care Med 39, 2550–2553, doi:10.1097/CCM.0b013e31822572fd (2011). [PubMed: 21705899]
15. Lockwood AH et al. The dynamics of ammonia metabolism in man. Effects of liver disease and hyperammonemia. J Clin Invest 63, 449–460, doi:10.1172/JCI109322 (1979). [PubMed: 429564]
16. Wolfe RR, Nelson RA, Wolfe MH & Rogers L Nitrogen cycling in hibernating bears. Proc. Amer. Soc. Mass Spectrometry 426 (1982).
17. Galster W & Morrison PR Gluconeogenesis in arctic ground squirrels between periods of hibernation. Am J Physiol 228, 325–330, doi:10.1152/ajplegacy.1975.228.1.325 (1975). [PubMed: 1147024]
18. Cotton CJ & Harlow HJ Avoidance of skeletal muscle atrophy in spontaneous and facultative hibernators. Physiol Biochem Zool 83, 551–560, doi:10.1086/650471 (2010). [PubMed: 20337528]
19. Deutz NEP, Thaden JJ, Ten Have GAM, Walker DK & Engelen M Metabolic phenotyping using kinetic measurements in young and older healthy adults. Metabolism 78, 167–178, doi:10.1016/j.metabol.2017.09.015 (2018). [PubMed: 28986165]
20. Vesali RF, Klaude M, Thunblad L, Rooyackers OE & Wernerman J Contractile protein breakdown in human leg skeletal muscle as estimated by [2H3]-3-methylhistidine: a new method. Metabolism 53, 1076–1080, doi:10.1016/j.metabol.2004.02.017 (2004). [PubMed: 15281022]
21. Laurent GJ Dynamic state of collagen: pathways of collagen degradation in vivo and their possible role in regulation of collagen mass. Am J Physiol 252, C1–9, doi:10.1152/ajpcell.1987.252.1.C1 (1987). [PubMed: 3544859]
22. Rennie MJ & Millward DJ 3-Methylhistidine excretion and the urinary 3-methylhistidine/creatinine ratio are poor indicators of skeletal muscle protein breakdown. Clin Sci (Lond) 65, 217–225, doi:10.1042/cs0650217 (1983). [PubMed: 6872456]
23. Epperson LE, Karimpour-Fard A, Hunter LE & Martin SL Metabolic cycles in a circannual hibernator. Physiol Genomics 43, 799–807, doi:10.1152/physiolgenomics.00028.2011 (2011). [PubMed: 21540299]
24. Gehrke S et al. Red Blood Cell Metabolic Responses to Torpor and Arousal in the Hibernator Arctic Ground Squirrel. J Proteome Res, doi:10.1021/acs.jproteome.9b00018 (2019).
25. D'Alessandro A, Nemkov T, Bogren LK, Martin SL & Hansen KC Comfortably Numb and Back: Plasma Metabolomics Reveals Biochemical Adaptations in the Hibernating 13-Lined Ground Squirrel. J Proteome Res 16, 958–969, doi:10.1021/acs.jproteome.6b00884 (2017). [PubMed: 27991798]
26. Moy RM Renal function in the hibernating ground squirrel Spermophilus columbianus. Am J Physiol 220, 747–753, doi:10.1152/ajplegacy.1971.220.3.747 (1971). [PubMed: 5545686]
27. Cynober LA Metabolic and Therapeutic Aspects of Amino Acids in Clinical Nutrition. 2nd edn, (CRC Press, 2003).
28. Deutz NE The 2007 ESPEN Sir David Cuthbertson Lecture: amino acids between and within organs. The glutamate-glutamine-citrulline-arginine pathway. Clin Nutr 27, 321–327, doi:10.1016/j.clnu.2008.03.010 (2008). [PubMed: 18501998]
29. Lesser RW, Moy R, Passmore JC & Pfeiffer EW Renal regulation of urea excretion in arousing and homeothermic ground squirrels (Citellus columbianus). Comp Biochem Physiol 36, 291–296, doi:10.1016/0010-406x(70)90009-5 (1970). [PubMed: 5515606]
30. Bell RA & Storey KB Regulation of liver glutamate dehydrogenase by reversible phosphorylation in a hibernating mammal. Comp Biochem Physiol B Biochem Mol Biol 157, 310–316, doi:10.1016/j.cbpb.2010.07.005 (2010). [PubMed: 20674762]
31. Thatcher BJ & Storey KB Glutamate dehydrogenase from liver of euthermic and hibernating Richardson's ground squirrels: evidence for two distinct enzyme forms. Biochem Cell Biol 79, 11–19 (2001). [PubMed: 11235914]
32. Spanaki C & Plaitakis A The role of glutamate dehydrogenase in mammalian ammonia metabolism. Neurotox Res 21, 117–127, doi:10.1007/s12640-011-9285-4 (2012). [PubMed: 22038055]

33. Wu G et al. Arginine metabolism and nutrition in growth, health and disease. Amino Acids 37, 153–168, doi:10.1007/s00726-008-0210-y (2009). [PubMed: 19030957]
34. Mugahid DA et al. Proteomic and Transcriptomic Changes in Hibernating Grizzly Bears Reveal Metabolic and Signaling Pathways that Protect against Muscle Atrophy. Sci Rep 9, 19976, doi:10.1038/s41598-019-56007-8 (2019). [PubMed: 31882638]
35. Lohuis TD, Beck TD & Harlow HJ Hibernating black bears have blood chemistry and plasma amino acid profiles that are indicative of long-term adaptive fasting. Canadian Journal of Zoology 9, 1257–1263 (2005).
36. Hissa R, Puukka M, Hohtola E, Sassi M & Risteli J Seasonal Changes in plasma nitrogenous compounds of the European brown bear (Ursus arctos arctos). Annales Zoologici Fennici 35, 205–213 (1998).
37. Harper AE, Miller RH & Block KP Branched-chain amino acid metabolism. Annu Rev Nutr 4, 409–454, doi:10.1146/annurev.nu.04.070184.002205 (1984). [PubMed: 6380539]
38. Abumrad NN, Wise KL, Williams PE, Abumrad NA & Lacy WW Disposal of alpha-ketoisocaproate: roles of liver, gut, and kidneys. Am J Physiol 243, E123–131, doi:10.1152/ajpendo.1982.243.2.E123 (1982). [PubMed: 7051844]
39. Sandovici M et al. Differential regulation of glomerular and interstitial endothelial nitric oxide synthase expression in the kidney of hibernating ground squirrel. Nitric Oxide 11, 194–200, doi:10.1016/j.niox.2004.08.002 (2004). [PubMed: 15491852]
40. Jani A et al. Kidney proteome changes provide evidence for a dynamic metabolism and regional redistribution of plasma proteins during torpor-arousal cycles of hibernation. Physiol Genomics 44, 717–727, doi:10.1152/physiolgenomics.00010.2012 (2012). [PubMed: 22643061]
41. Nelson RA & Jones JD Leucine Metabolism in the Black Bear. A Selection of Papers from the Seventh International Conference on Bear Research and Management, 329–331 (1986).
42. Metges CC et al. Incorporation of urea and ammonia nitrogen into ileal and fecal microbial proteins and plasma free amino acids in normal men and ileostomates. Am J Clin Nutr 70, 1046–1058, doi:10.1093/ajcn/70.6.1046 (1999). [PubMed: 10584050]
43. Nelson DL & Cox MM Lehninger Principles of Biochemistry. 5th edn, (W.H. Freeman, 2008).
44. Millward DJ et al. The transfer of 15N from urea to lysine in the human infant. Br J Nutr 83, 505–512 (2000). [PubMed: 10953675]
45. Drew KL et al. Ascorbate and glutathione regulation in hibernating ground squirrels. Brain Res 851, 1–8 (1999). [PubMed: 10642822]
46. Fenves AZ, Kirkpatrick HM 3rd, Patel VV, Sweetman L & Emmett M Increased anion gap metabolic acidosis as a result of 5-oxoproline (pyroglutamic acid): a role for acetaminophen. Clin J Am Soc Nephrol 1, 441–447, doi:10.2215/CJN.01411005 (2006). [PubMed: 17699243]
47. Yu YM et al. Plasma L-5-oxoproline kinetics and whole blood glutathione synthesis rates in severely burned adult humans. Am J Physiol Endocrinol Metab 282, E247–258, doi:10.1152/ajpendo.00206.2001 (2002). [PubMed: 11788355]
48. D'Alessandro A et al. Trauma/hemorrhagic shock instigates aberrant metabolic flux through glycolytic pathways, as revealed by preliminary (13)C-glucose labeling metabolomics. J Transl Med 13, 253, doi:10.1186/s12967-015-0612-z (2015). [PubMed: 26242576]
49. Koga M et al. Glutathione is a physiologic reservoir of neuronal glutamate. Biochem Biophys Res Commun 409, 596–602, doi:10.1016/j.bbrc.2011.04.087 (2011). [PubMed: 21539809]
50. Kumar A & Bachhawat AK Pyroglutamic acid: throwing light on a lightly studied metabolite. Current Science 102, 288–297 (2012).
51. Griffith OW, Bridges RJ & Meister A Transport of gamma-glutamyl amino acids: role of glutathione and gamma-glutamyl transpeptidase. Proc Natl Acad Sci U S A 76, 6319–6322, doi:10.1073/pnas.76.12.6319 (1979). [PubMed: 42913]
52. Stevenson TJ, Duddleston KN & Buck CL Effects of season and host physiological state on the diversity, density, and activity of the arctic ground squirrel cecal microbiota. Appl Environ Microbiol 80, 5611–5622, doi:10.1128/AEM.01537-14 (2014). [PubMed: 25002417]
53. Kondo H, Miura M & Itokawa Y Antioxidant enzyme systems in skeletal muscle atrophied by immobilization. Pflugers Arch 422, 404–406 (1993). [PubMed: 8437891]

54. Wickler SJ, Hoyt DF & van Breukelen F Disuse atrophy in the hibernating golden-mantled ground squirrel, Spermophilus lateralis. Am J Physiol 261, R1214–1217, doi:10.1152/ajpregu.1991.261.5.R1214 (1991). [PubMed: 1951770]
55. Bodine SC Hibernation: the search for treatments to prevent disuse-induced skeletal muscle atrophy. Exp Neurol 248, 129–135, doi:10.1016/j.expneurol.2013.06.003 (2013). [PubMed: 23769906]
56. James RS, Staples JF, Brown JC, Tessier SN & Storey KB The effects of hibernation on the contractile and biochemical properties of skeletal muscles in the thirteen-lined ground squirrel, Ictidomys tridecemlineatus. J Exp Biol 216, 2587–2594, doi:10.1242/jeb.080663 (2013). [PubMed: 23531815]
57. Lee K et al. Overcoming muscle atrophy in a hibernating mammal despite prolonged disuse in dormancy: proteomic and molecular assessment. J Cell Biochem 104, 642–656, doi:10.1002/jcb.21653 (2008). [PubMed: 18181155]
58. Lohuis TD, Harlow HJ & Beck TD Hibernating black bears (Ursus americanus) experience skeletal muscle protein balance during winter anorexia. Comp Biochem Physiol B Biochem Mol Biol 147, 20–28, doi:10.1016/j.cbpb.2006.12.020 (2007). [PubMed: 17307375]
59. Goropashnaya AV, Barnes BM & Fedorov VB Transcriptional changes in muscle of hibernating arctic ground squirrels (Urocitellus parryii): implications for attenuation of disuse muscle atrophy. Sci Rep 10, 9010, doi:10.1038/s41598-020-66030-9 (2020). [PubMed: 32488149]
60. Hindle AG et al. Prioritization of skeletal muscle growth for emergence from hibernation. J Exp Biol 218, 276–284, doi:10.1242/jeb.109512 (2015). [PubMed: 25452506]
61. Regan MD et al. Shifts in metabolic fuel use coincide with maximal rates of ventilation and body surface rewarming in an arousing hibernator. Am J Physiol Regul Integr Comp Physiol 316, R764–R775, doi:10.1152/ajpregu.00379.2018 (2019). [PubMed: 30969844]
62. Perez-Pinzon MA, Gidday JM & Zhang JH Innate Tolerance in the CNS: Translational Neuroprotection by Pre- and Post-Conditioning. (Springer Science +Business Media New York, 2013).
63. van Breukelen F & Martin SL Translational initiation is uncoupled from elongation at 18 degrees C during mammalian hibernation. Am J Physiol Regul Integr Comp Physiol 281, R1374–1379, doi:10.1152/ajpregu.2001.281.5.R1374 (2001). [PubMed: 11641105]
64. Laurent MR et al. Muscle-bone interactions: From experimental models to the clinic? A critical update. Mol Cell Endocrinol 432, 14–36, doi:10.1016/j.mce.2015.10.017 (2016). [PubMed: 26506009]
65. Kornfeld SF, Biggar KK & Storey KB Differential expression of mature microRNAs involved in muscle maintenance of hibernating little brown bats, Myotis lucifugus: a model of muscle atrophy resistance. Genomics Proteomics Bioinformatics 10, 295–301, doi:10.1016/j.gpb.2012.09.001 (2012). [PubMed: 23200139]
66. Secombe P, Harley S, Chapman M & Aromataris E Feeding the critically ill obese patient: a systematic review protocol. JBI Database System Rev Implement Rep 13, 95–109, doi:10.11124/jbisrir-2015-2458 (2015).
67. Wolfe RR & Chinkes DL Isotope Tracers in Metabolic Research: Principles and Practice of Kinetic Analysis 2nd edn, (Wiley, 2005).
68. Mason A, Engelen M, Ivanov I, Toffolo GM & Deutz NEP A four-compartment compartmental model to assess net whole body protein breakdown using a pulse of phenylalanine and tyrosine stable isotopes in humans. Am J Physiol Endocrinol Metab 313, E63–E74, doi:10.1152/ajpendo.00362.2016 (2017). [PubMed: 28270442]
69. Moore HB et al. The metabolic time line of pancreatic cancer: Opportunities to improve early detection of adenocarcinoma. Am J Surg 218, 1206–1212, doi:10.1016/j.amjsurg.2019.08.015 (2019). [PubMed: 31514959]
70. Nemkov T, Reisz JA, Gehrke S, Hansen KC & D'Alessandro A High-Throughput Metabolomics: Isocratic and Gradient Mass Spectrometry-Based Methods. Methods Mol Biol 1978, 13–26, doi:10.1007/978-1-4939-9236-2_2 (2019). [PubMed: 31119654]
71. Kanehisa M The KEGG database. Novartis Found Symp 247, 91–101; discussion 101-103, 119-128, 244-152 (2002). [PubMed: 12539951]

72. Kanehisa M & Goto S KEGG: kyoto encyclopedia of genes and genomes. Nucleic Acids Res 28, 27–30, doi:10.1093/nar/28.1.27 (2000). [PubMed: 10592173]

73. Nemkov T, Hansen KC & D'Alessandro A A three-minute method for high-throughput quantitative metabolomics and quantitative tracing experiments of central carbon and nitrogen pathways. Rapid Commun Mass Spectrom 31, 663–673, doi:10.1002/rcm.7834 (2017). [PubMed: 28195377]

74. Williams CT et al. Hibernating above the permafrost: effects of ambient temperature and season on expression of metabolic genes in liver and brown adipose tissue of arctic ground squirrels. J Exp Biol 214, 1300–1306, doi:10.1242/jeb.052159 (2011). [PubMed: 21430207]

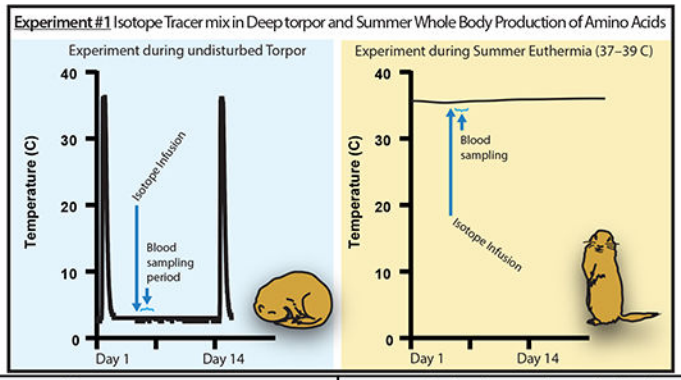

Tracer	Pulse tracer (nmol/g body weight)
Citrulline (5-^{13}C; 4,4,5,5-D4)	0.79 (±0.04)
Ornithine ($^{13}C_5$)	0.40 (±0.02)
Glutamine ($^{15}N_2$)	3.14 (±0.15)
Glutamic acid (1,2-$^{13}C_2$)	3.81 (±0.19)
Glycine (1-^{13}C)	9.65 (±0.48)
Leucine ($^{13}C_6$)	2.27 (±0.11)
Tau-Methylhistidine (Methyl-D3)	0.18 (±0.01)
trans-4-Hydroxy-L-proline (2,5,5-D3)	0.35 (±0.02)
Phenylalanine (Ring-$^{13}C_6$)	4.73 (±0.23)
Taurine (1,2-$^{13}C_2$)	1.67 (±0.08)
Tryptophan (Indole-D5)	1.44 (±0.07)
Tyrosine (Ring-D4)	0.40 (±0.02)
Isoleucine (1-^{13}C)	0.21 (±0.01)
Valine ($^{13}C_5$)	1.02 (±0.05)
Ketoisocaproic acid (KIC, 1-^{13}C)	1.49 (±0.07)
Ketoisovaleric acid (KIV, Dimethyl-$^{13}C_2$)	1.61 (±0.08)
Keto-β-methylvalerate (KMV, $^{13}C_6$)	1.16 (±0.06)
β-hydroxy β-methylbutric acid (HMB, 3,4 methyl $^{13}C_2$)	0.08 (±0.00)

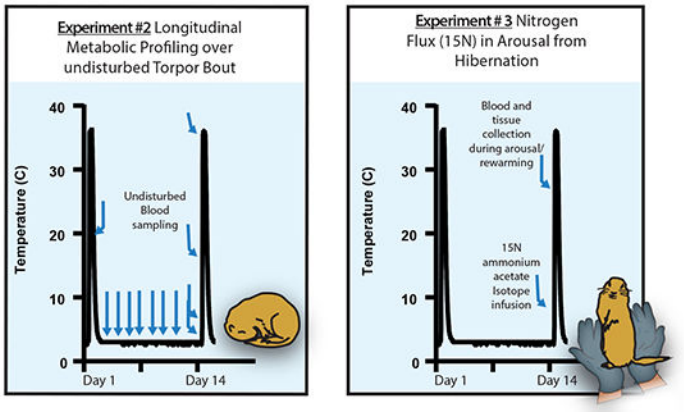

Figure 1.

Schematic for separate experimental procedures. Experiment #1 infused amino acid isotopes and sampled blood without inducing arousal, body temperature (T_b) <4°C represents torpor, T_b >34°C represents interbout arousal. Experiments were repeated in the same animals during summer euthermia in the post-absorptive state. Composition of isotope pulse infusion in deep torpor and summer euthermic animals during experiment #1 reported in nmol/g body weight, n=14 AGS, mean ±SEM. Experiment #2 sampled blood in undisturbed hibernators

from entrance into hibernation through a full torpor bout. Experiment #3 induced arousal by handling animals, infused ^{15}N ammonium acetate and collected blood and tissues.

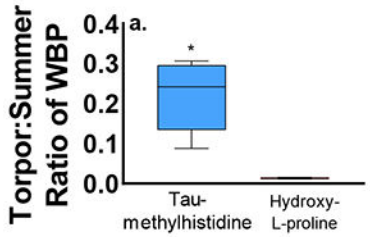

Metabolite	Summer Euthermic WBP (SEM) (nmol/g weight/h)	Torpor WBP (SEM) (nmol/g weight/h)
Hydroxy L-Proline	8.27 (1.33)	0.13 (0.02)*
Tau-methylhistidine	1.83 (0.19)	0.41 (0.08)*

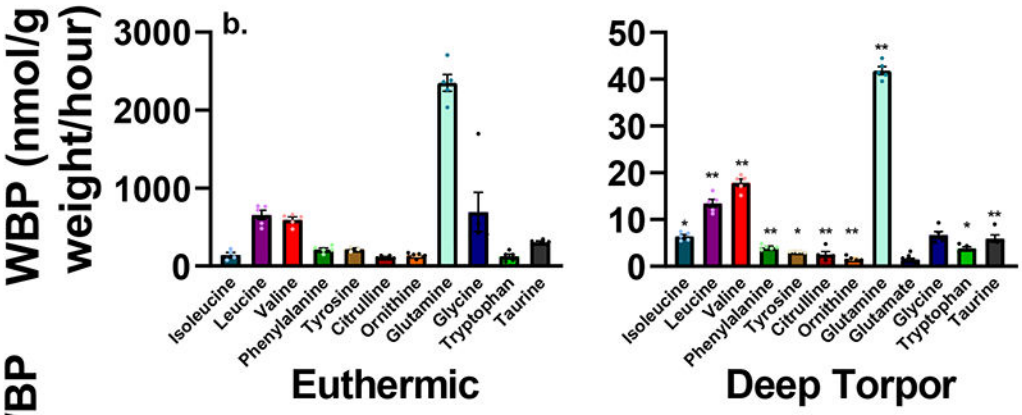

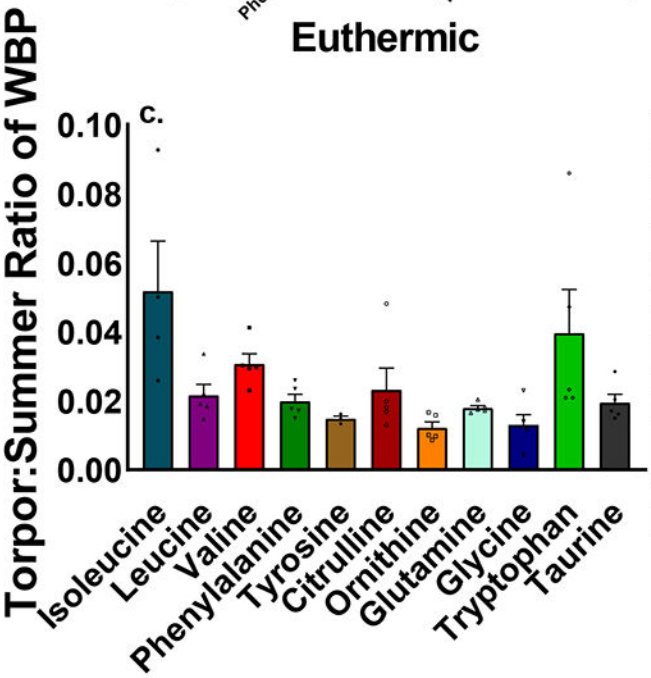

d.

Tau-methylhistidine Regression Analysis					
Metabolite	R^2	Intercept	Slope	F	*p*
Phenylalanine	0.585*	-0.303	0.155	9.869	**0.016**
Tyrosine	0.198	0.223	0.040	1.731	0.23
Leucine	0.204	0.146	0.014	1.790	0.223
Valine	0.320	-0.037	0.021	3.301	0.112
Citrulline	0.456*	0.152	0.075	5.866	**0.046**
Ornithine	0.016	0.355	0.037	0.116	0.743
Glutamine	0.523*	-0.107	0.011	7.670	**0.028**
Glutamate	0.294	0.180	0.159	2.908	0.132
Glycine	0.400	0.077	0.039	4.661	0.068
Hydroxy-L-Proline	0.428	-0.012	3.353	5.239	0.056
Taurine	0.109	0.187	0.031	0.852	0.387
Tryptophan	0.320	-0.205	0.180	3.295	0.112

Figure 2.

Skeletal muscle breakdown is on-going and whole body production (WBP) of all metabolites are depressed in deep torpor. **a.** In deep torpor, tau-methylhistidine (3-MH), a marker of skeletal muscle breakdown, is less repressed than hydroxy L-proline (hPRO), a marker of collagen breakdown (*p<0.001, WBP ratio hPRO vs 3-MH, two tailed t-test, boxplot whiskers represent min-max value, centre line represents the median and box boundaries represent 25th and 75th percentiles). Table insert: 3-MH and hPRO both significantly decline during torpor (n=9 AGS) compared to summer (n=5 AGS) (*p<0.001, two tailed t-test). **b.** Whole body production (WBP) of all metabolites are depressed in

torpor compared to summer euthermia (n=5 AGS for all metabolites excluding tyrosine n=3 AGS and isoleucine n=4 AGS). WBP of glutamate in summer was too fast to generate a reliable decay curve and is not reported. (*p<0.05, **p<0.001 euthermic vs. deep torpor, paired two tailed t-test, FDR corrected; phenylalanine, leucine, valine, citrulline, glutamine, taurine p=0.000, tyrosine p=0.007, isoleucine p=0.023, ornithine p=0.001, glycine p=0.053, tryptophan p=0.011). **c.** WBP of amino acids is suppressed to varying degrees (torpor:summer WBP ratio, n=5 AGS). **d.** Linear regression analysis for tau-methylhisitidine WBP compared to metabolite WBP in deep torpor. Phenylalanine, glutamine and citrulline WBP are significantly correlated to tau-methylhistidine WBP in torpor (p<0.05, linear regression, n=9 AGS). Data shown are mean ±SEM

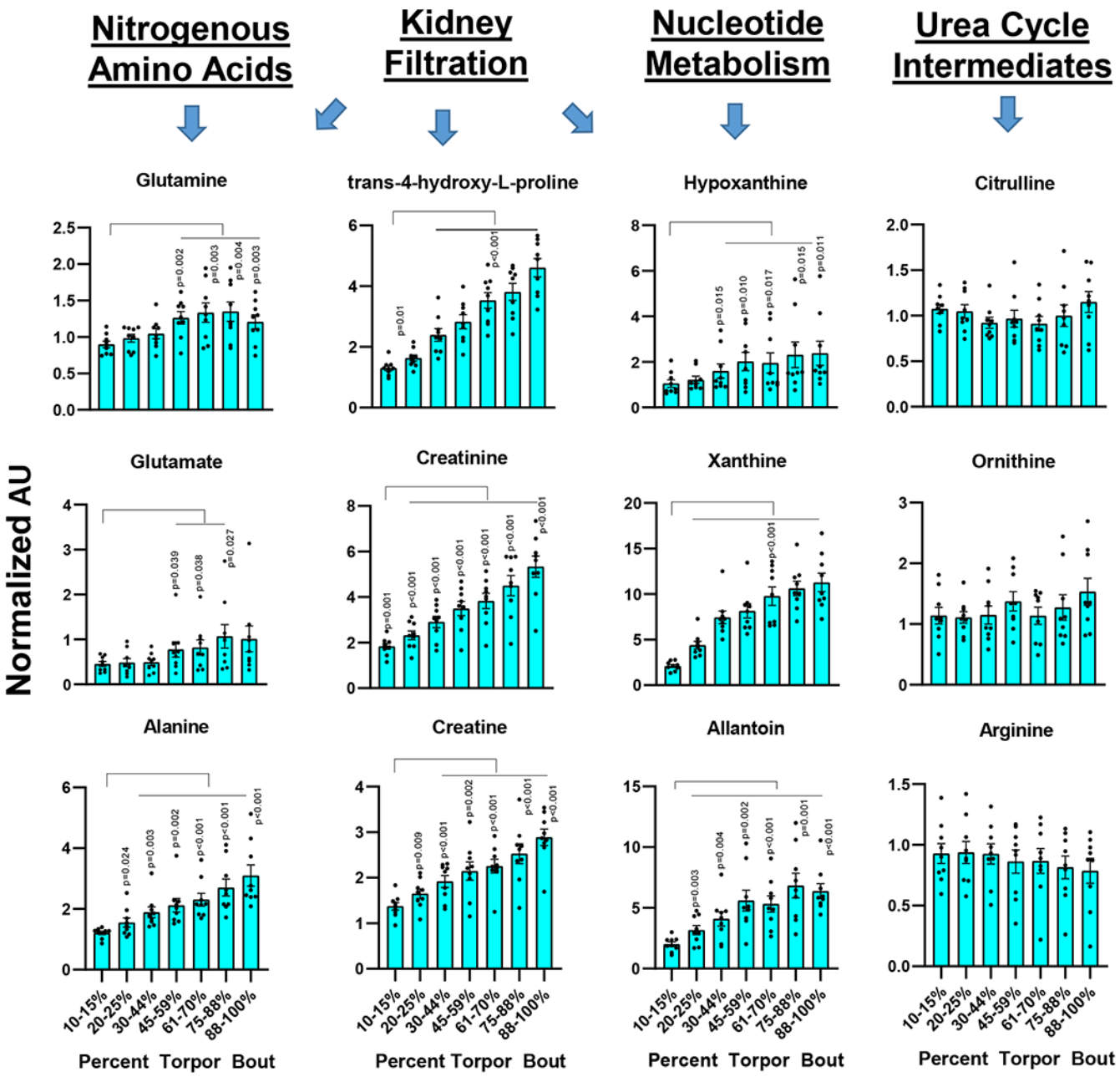

Figure 3.

Circulating nitrogen metabolite pools increase as torpor progresses while urea cycle intermediates do not increase. Data shown are relative abundance normalized to a sample collected at entrance into torpor at a T_b of 11-12°C. The x-axis indicates duration of the torpor bout expressed as a percent of the total length of the bout in days. (p values compare specific time points in the torpor bout vs early torpor (10- 15%) posthoc LSD two-sided, n=9 AGS). Creatinine, creatine, trans-4-hydroxy-L-proline, allantoin, hypoxanthine, xanthine significantly increase over torpor (p values represent specific time points in the torpor bout vs early torpor (10- 15%) posthoc LSD two-sided, n=9 AGS). Urea cycle intermediates citrulline, ornithine and arginine do not increase over torpor (ns, repeated measures

ANOVA). Measurements are from individual animals sampled over a single, undisturbed torpor bout. Data shown as mean ±SEM

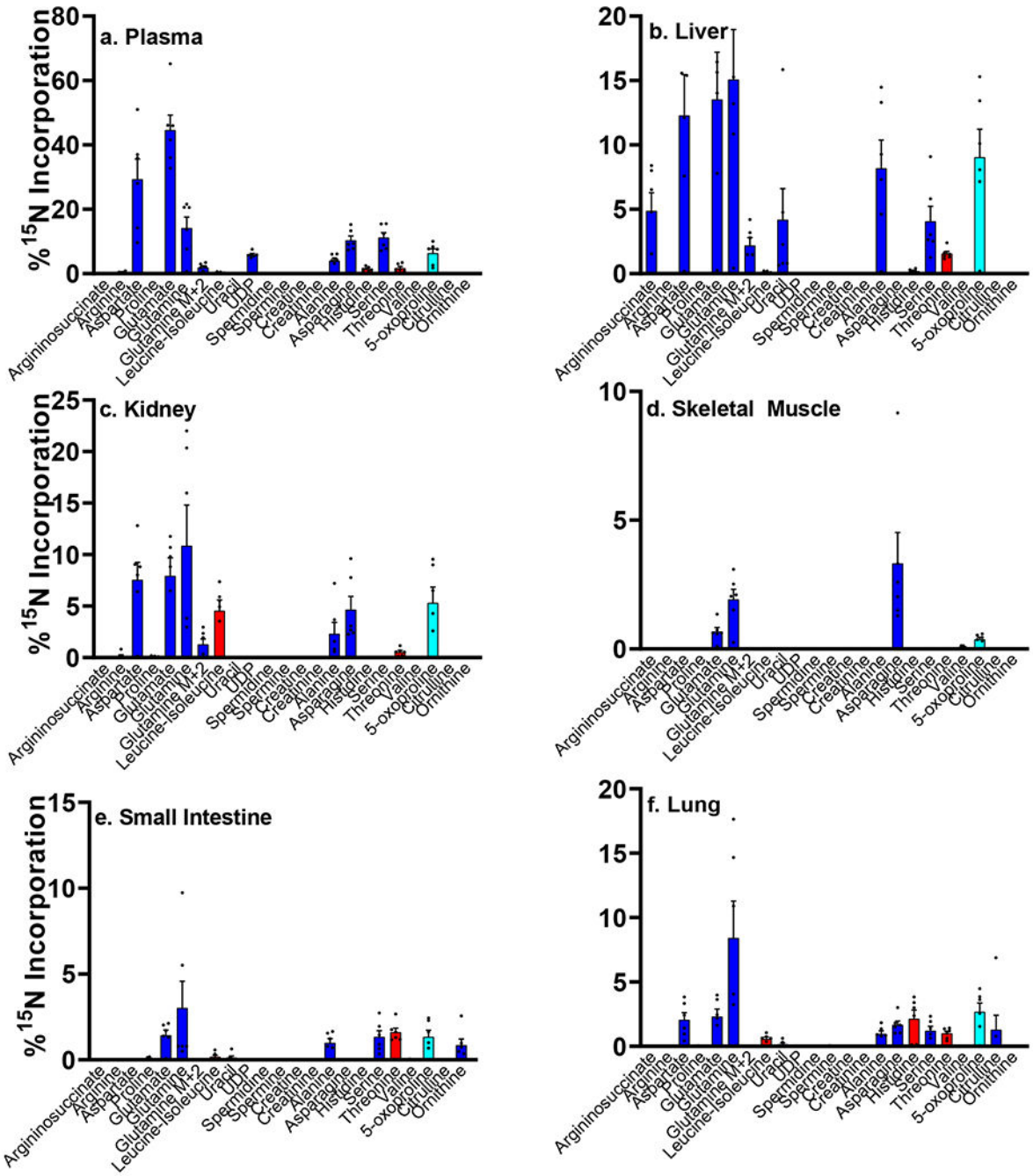

Figure 4.

Free ^{15}N ammonia is recycled into nonessential amino acids (blue), essential amino acids (red) and 5-oxoproline (turquoise) during arousal from torpor. Data show percent of ^{15}N incorporation during arousal from torpor following 72 mg/kg ^{15}N ammonium acetate pulse infusion, n=6, mean ±SEM. Calculations for percent ^{15}N incorporation: (^{15}N metabolite peak area)/(^{15}N metabolite peak area + ^{14}N metabolite peak area)*100 following natural abundance correction.

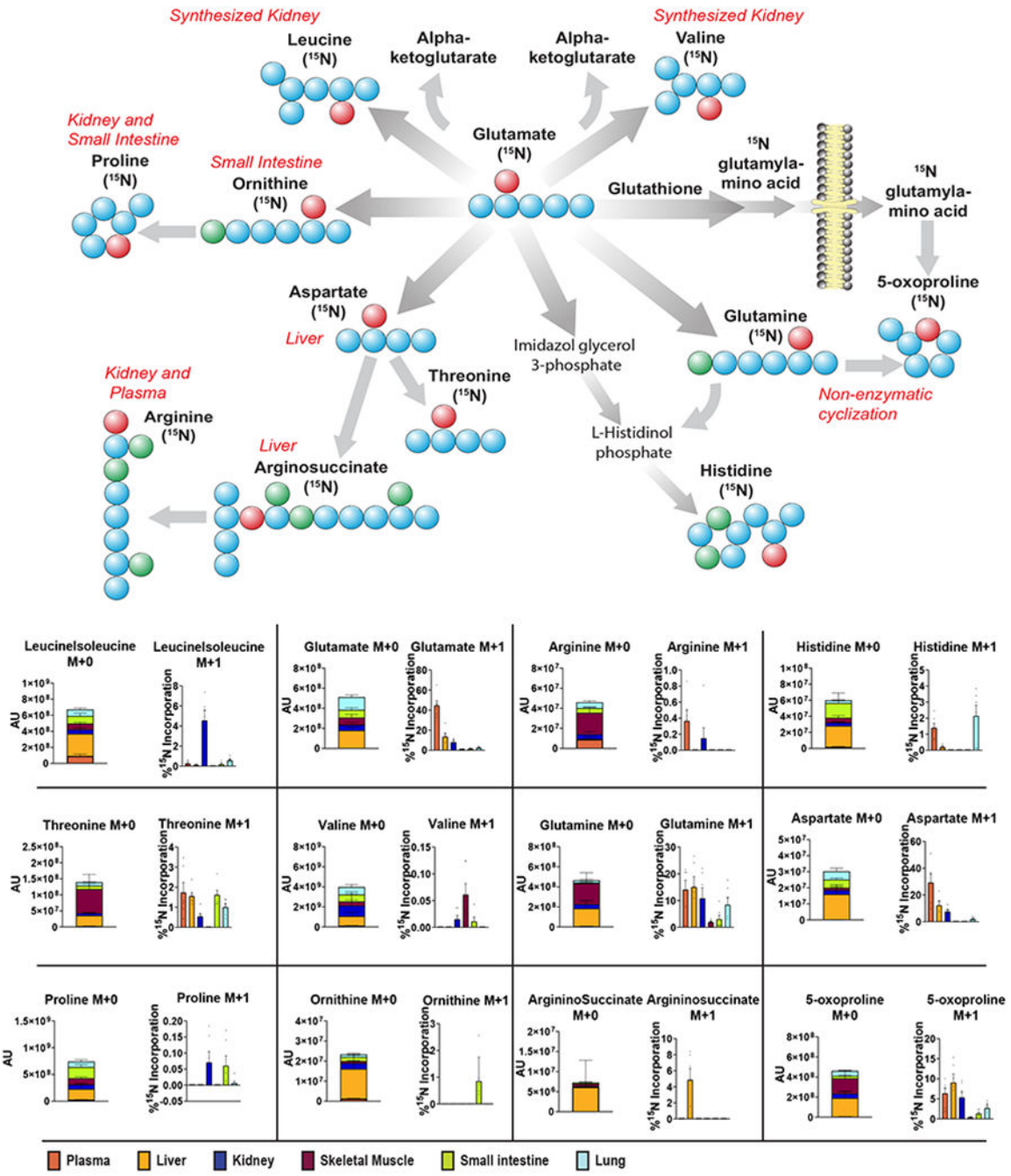

Figure 5.

Proposed pathway for 15N ammonia recycling into amino acids depends on non-essential amino acid incorporation during arousal from torpor. Unlabeled metabolites (14N), denoted as M+0, measured in the pulse experiments are shown in stacked bar graphs (72 mg/kg 15N ammonium acetate pulse infusion n=6). Bar graphs show percent of 15N incorporation (M +1) into metabolites (72 mg/kg 15N ammonium acetate pulse infusion, n=6). Percent 15N incorporation (denoted as M+1) calculated as: ((15N metabolite peak area/(15N metabolite peak area + 14N metabolite peak area))*100 following natural abundance correction.

Suggested location of 15N nitrogen is labeled by red circles, but analysis cannot determine specific location in metabolite. Carbon is labeled by blue circles, unlabeled nitrogen by green circles. Data shown mean ±SEM

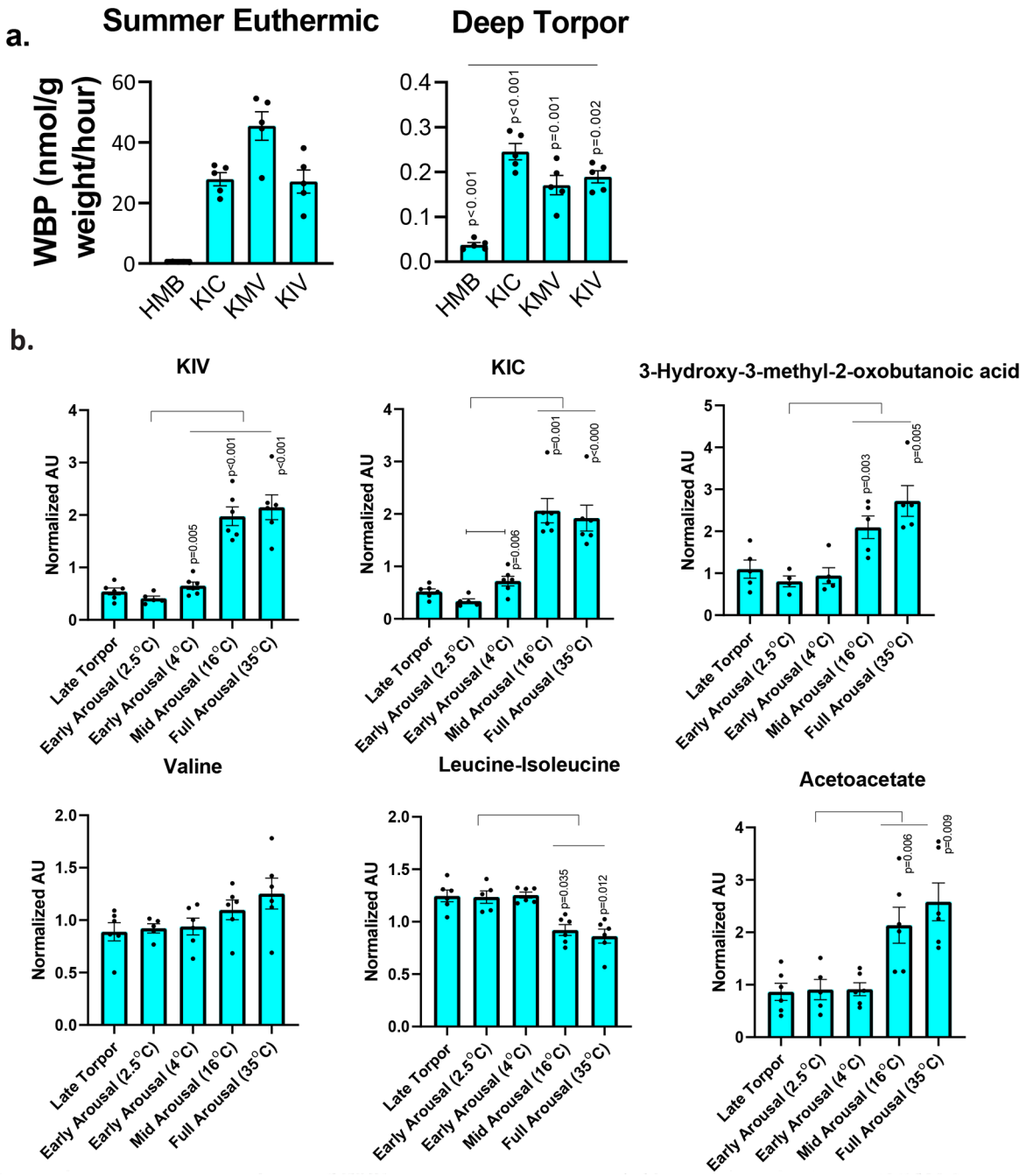

Figure 6: Branched chained ketoacid WBP is suppressed in torpor, but ketoacids and ketones increase during arousal from torpor.

a.) Ketoisocaproic acid (KIC), ketoisovalerate (KIV), keto-beta-methylvalerate (KMV) and betahydroxy-beta-methylbutyrate (HMB) whole body production (WBP) are suppressed in torpor compared to summer euthermia (**p<0.002, WBP torpor vs. WBP summer euthermic, paired two tailed t-test, n=5 AGS). **b.)** KIC, KIV, 3- hydroxy-3-methyl-2-oxobutanoic acid and acetoacetate increase over arousal (p values compare specific time points vs early arousal (2.5°C), posthoc LSD two-sided, n=6 AGS). Valine does not

significantly increase over arousal (ns, repeated measures ANOVA) and leucine-isoleucine decreases (*p<0.05 vs early arousal (2.5°C), posthoc LSD, n=6 AGS). Measurements are from individual animals sampled over a natural arousal. Measurements are normalized to the relative abundance of sample collected during entrance into hibernation at T_b 11-12°C. Data shown as mean ±SEM

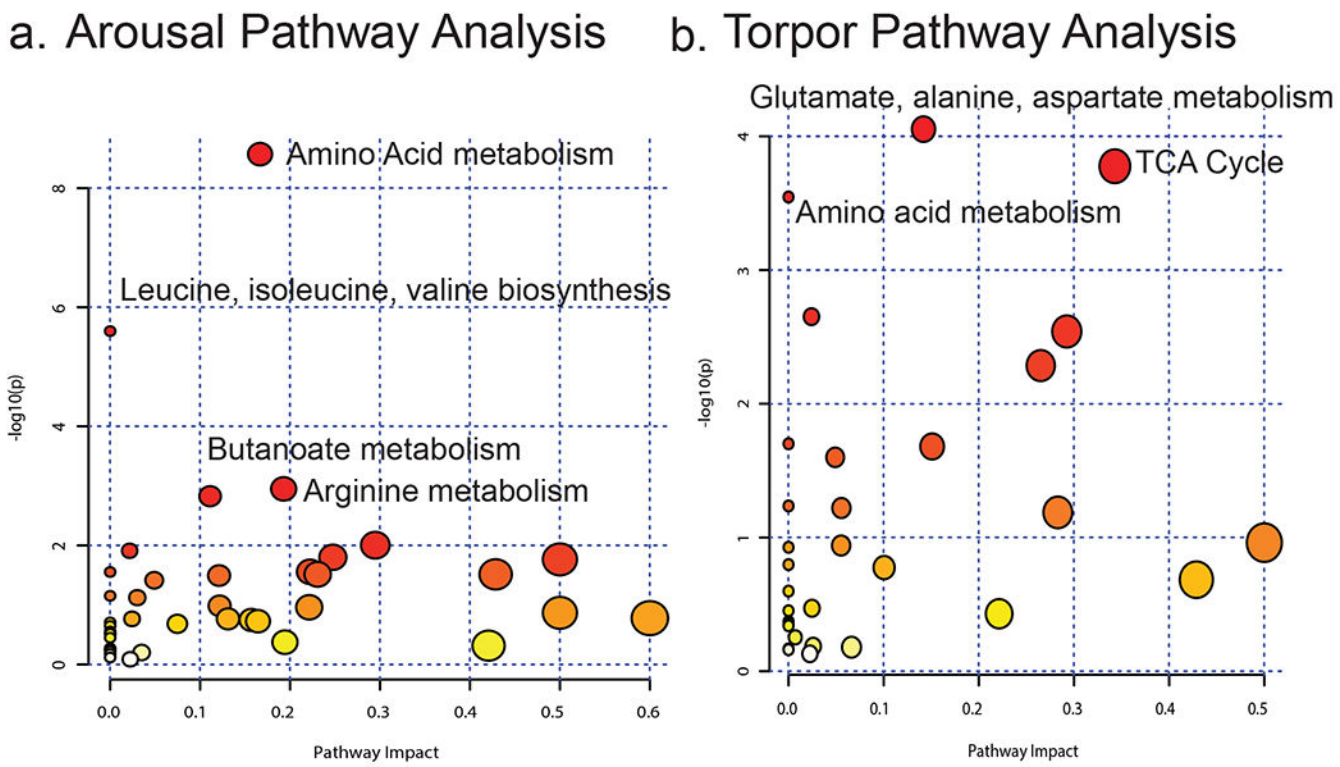

Figure 7:

Pathway enrichment analysis shows evidence for amino acid metabolism and branched chain amino acid biosynthesis in arousal from torpor, and points to the prevalence of transamination reactions involving glutamate, alanine and aspartate during torpor. **a.)** Arousal pathway enrichment analysis compared early arousal (2.5°C) and full arousal (35°C) using MetaboAnalyst 4.0 (n=6) **b.)** Torpor pathway enrichment analysis compared early torpor (10-15% of torpor bout completed) to late torpor (88-100% of torpor bout completed) using MetaboAnalyst 4.0 (n=9)